AD-A160 538 PILOTED SIMULATION OF ONE-ON-ONE HELICOPTER AIR COMBAT AT NOE (NAP-OF-THE..(U) NATIONAL AERONAUTICS AND SPACE ADMINISTRATION MOFFETT FIELD C.. M S LEWIS ET AL. 1/1

UNCLASSIFIED APR 85 NASA-A-85130 NASA-TM-86686 F/G 1/2 NL

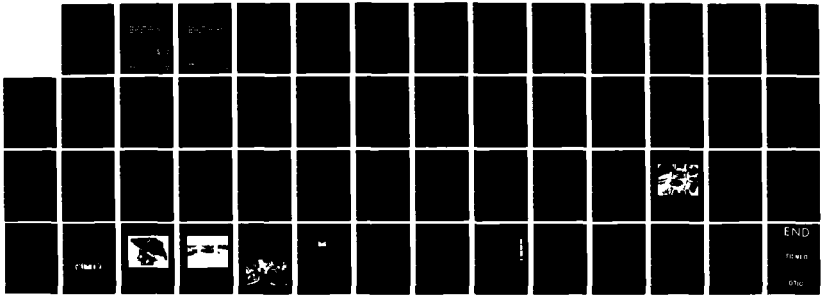

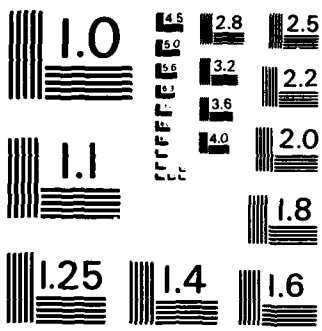

NASA Technical Memorandum 86686

USAAVSCOM Technical Report 85-A-2

Piloted Simulation of One-On-One Helicopter Air Combat at NOE Flight Levels

Michael S. Lewis and Edwin W. Aiken

April 1985

NASA
National Aeronautics and Space Administration

United States Army Aviation Systems Command

85 10 23 014

NASA Technical Memorandum 86686

USAAVSCOM Technical Report 85-A-2

Piloted Simulation of One-On-One Helicopter Air Combat at NOE Flight Levels

Michael S. Lewis
Edwin W. Aiken, Aeromechanics Laboratory, U. S. Army Research and Technology Laboratories-AVSCOM, Ames Research Center, Moffett Field, California

April 1985

National Aeronautics and Space Administration

Ames Research Center
Moffett Field, California 94035

United States Army
Aviation Systems
Command
St. Louis, Missouri 63120

SYMBOLS AND ABBREVIATIONS

AXP	longitudinal acceleration at the pilot station
AYP	lateral acceleration at the pilot station
AZP	vertical acceleration at the pilot station
e	hinge offset, %
PB	computer mnemonic for p
PK	probability of kill
PSR	probability of survival, red aircraft
PSB	probability of survival, blue aircraft
p	roll rate about body axis, deg/sec
QB	computer mnemonic for q
q	pitch rate about body axis, deg/sec
RB	computer mnemonic for r
r	yaw rate about body axis, deg/sec
Veq	airspeed, knots
ϕ	roll angle, deg
θ	pitch angle, deg
k_β	flapping hinge restraint, ft-lb/rad
γ	lock number

Acronyms

ACM	air combat maneuvering
CGI	Computer Generated Imagery
DIG	digital image generator
HUD	head-up display
NOE	nap-of-the-earth
PMD	panel-mounted display

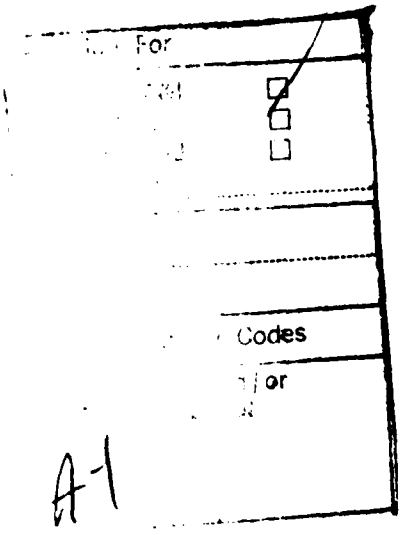

SCAS Stability and Control Augmentation System

VMS Vertical Motion Simulator

A PILOTED SIMULATION OF ONE-ON-ONE HELICOPTER AIR COMBAT AT NOE FLIGHT LEVELS

Michael S. Lewis and Edwin W. Aiken
Aeromechanics Laboratory
U.S. Army Research and Technology Laboratories, AVSCOM
NASA Ames Research Center, Moffett Field, California

1. SUMMARY

A piloted simulation designed to examine the effects of terrain proximity and control system design on helicopter performance during one-on-one air combat maneuvering (ACM) is discussed. The NASA Ames Vertical Motion Simulator (VMS) and Computer Generated Imagery (CGI) systems were modified to allow two aircraft to be independently piloted on a single CGI data base. Engagements were begun with the blue aircraft already in a tail-chase position behind the red and also with the two aircraft originating from positions unknown to each other. Maneuvering was very aggressive and safety requirements for minimum altitude, separation, and maximum bank angles typical of flight test were not used. Results indicate that the presence of terrain features adds an order of complexity to the task performance over clear air ACM and that a mix of attitude and rate command-type Stability and Control Augmentation System (SCAS) design may be desirable. The simulation system design, the flight paths flown, and the tactics used were compared favorably by the evaluation pilots to actual flight test experiments.

2. INTRODUCTION

The Army has recently recognized the need to provide its helicopters with the capability to engage both helicopter and fixed-wing threats. In January of 1982, a U.S. Army Aviation Mission Area Analysis Report identified helicopter air-to-air and air defense suppression capabilities as the first priority deficiency of Army aviation.

Flight tests and crew training have been in progress for some time. The U.S. Marine Corps Marine Aviation Weapons and Tactics Squadron One (MAWTS 1) has been training senior Marine and U.S. Navy pilots since 1978 in the most effective use of their current aircraft and weapons. As part of this training, MAWTS instructs pilots in helicopter-vs-helicopter evasive maneuvering.

Due to a lack of flight test data on the subject of helicopter air combat maneuvering, the U.S. Army Applied Technology Laboratory has undertaken a series of instrumented flight tests at the Naval Air Test Center, Patuxent River, MD. In April 1983, Phase I of the Air-to-Air Combat Test (AACT I) was conducted utilizing OH-58 and AH-1S aircraft. In July 1983, Phase II flights were completed utilizing Sikorsky S-76 and UH-60 aircraft (ref. 1). From May 1978 through February 1979, the Army and U.S. Air Force also conducted a series of flight tests involving current Army aircraft against Air Force fixed-wing threats (J-CATCH). In addition, members of the Third Squadron, Fifth Cavalry located at Ft. Lewis, WA, have been working since August 1982 to develop a Rotary Wing Air Combat Maneuvering Guide to standardize Army

air combat training and tactics (ref. 2). In all of these flight tests, safety restrictions for minimum altitude, roll attitude, and relative range are required.

Digital simulation studies to date have included work by Flight Systems, Incorporated, and Grumman Aerospace Corporation, among others (refs. 3 and 4). These non-real-time studies have investigated topics concerning the air-to-air combat effectiveness of helicopters; the impact of flying qualities on mission effectiveness; and the impact of speed, maneuverability, and armament for LHX design concepts. None of these simulations included a pilot in the loop or any sort of sophisticated visual terrain model. Fixed-wing manned simulators in Government and industry have not lent themselves easily to helicopter engagements because of aircraft modeling complexities and the lack of high-fidelity low-level visual scene generating systems.

Since Army aircraft frequently operate at nap-of-the-earth (NOE) altitudes, encounters with threat aircraft are likely to occur at this low level. It was desired, therefore, to design a simulation system which would allow the effects of terrain to be included in an investigation of helicopter air combat maneuvering without the safety restrictions necessary in flight tests. The helicopter modeling capability, wide field-of-view CGI display, and the large motion travel of the NASA Ames Research Center VMS were well suited for this task, although new system capabilities were required.

These new capabilities included a dual-eyepoint CGI real time software program which allowed for two independently maneuverable views of a common visual data base. The data base itself was specially designed for this project, as was a system of head-up and panel-mounted information displays. The red aircraft pilot station and equations of motion were new, as were a weapons model and scoring algorithm. These systems are described fully in the Facilities section below.

A number of people contributed invaluable expertise and support toward the development and conduct of this experiment. Their time and efforts are gratefully noted. Dennis Yeo, Software Systems, Inc.; Matt Blake, SYRE, Inc.; Russ Sansom, SYRE, Inc.; Arnie Estep, SYRE, Inc.; and Mehra Heravi, SYRE, Inc.

3. EXPERIMENTAL DESIGN

To investigate the handling qualities requirements necessary for NOE air combat maneuvering, a simulation measuring combat performance and eliciting pilot comments was conducted. Experimental variables included rotor hub type, basic SCAS design, initial altitude, initial position, target aggressiveness, and weapon parameters.

The rotor hub model and SCAS parameters of the blue aircraft were varied to represent a sample of the teetering, articulated, and hingeless design configurations of a previous NOE handling qualities experiment using the NASA-developed ARMCOP helicopter math model. (Details of the configuration types and the ARMCOP model are found in refs. 5, 6, and 7.) In general, the ARMCOP model consists of equations for the separate aerodynamic force and moment contributions of the main rotor, tail rotor, fuselage, fin, and horizontal stabilizer. For this simulation, the aerodynamics of the fuselage and empennage and the inertias were based on the characteristics of the AH-1G Cobra Helicopter.

The characteristics of the configurations chosen are shown in tables 1-4, along with an identifier for those used in references 5 and 6. The hub type was set by the value of hinge offset (zero for a teetering hub, 5% for articulated, 14% for hingeless). The SCAS type was also varied from a rate command system (A204, B11) to an attitude command system (T05). Configurations T05 and B11 had augmentation to minimize pitch and yaw coupling to collective inputs. A listing of the stability and control derivatives for each configuration is provided in tables 5-9.

In order to evaluate the effects of terrain on air combat maneuvering, the initial altitude of the two aircraft was varied from clear-air (1000 ft) to low-level (200 ft). The initial position was also varied. Early in the experiment, the blue aircraft started each run at the same altitude and 1000 ft behind the red. Later, however, free engagements were conducted with the two aircraft starting from random positions in the visual data base unknown to each other.

A fundamental factor in air combat maneuvering is the unpredictability of the opponent aircraft. This factor, however, makes an ACM experiment design and data analysis somewhat more difficult than an exactly repeatable and more controlled task. A general effort was made, though, to keep the target level of aggressiveness fairly consistent during the configuration evaluation engagements prior to free maneuvering. Three levels of target maneuvering were chosen. "Gentle" maneuvering consisted of small roll and pitch attitude changes (±20° and ±10°, respectively) in clear air. "Hard" maneuvering involved larger variations (±80° roll and ±20° pitch). "NOE" maneuvering was the most aggressive, largely because of the proximity of terrain obstacles which both aircraft needed to avoid.

Weapon parameters were also varied. Gun range and firing cone for each aircraft (fig. 1) were nominally set to a maximum of 750 ft and ±2° in pitch and azimuth, respectively. The effects of increasing the range up to 2000 ft or decreasing the firing cone to ±1° were briefly examined.

4. CONDUCT OF THE EXPERIMENT

4.1 Facilities

Vertical motion simulator- The simulation was conducted using the NASA Ames six degree-of-freedom VMS for the blue aircraft (fig. 2). The VMS was designed to provide extensive cockpit motion to aid in the study of handling qualities of existing or proposed aircraft (ref. 8). The primary inputs from the aircraft math model to the motion system software are the body axis accelerations sensed by the pilot, AXP, AYP, AZP, and the aircraft body axis rotational rates PB, QB, RB. These six inputs are subjected to second-order washout filters characterized by a frequency and high frequency gain. For this experiment the hexapod-mounted interchangeable cab was equipped with a single pilot cockpit and a three-window, wide field-of-view CGI visual display (fig. 3).

Motion system gains and frequencies were set to allow for maximum travel without exceeding system limits during the large amplitude maneuvers performed (table 11). Cab orientation on the hexapod base was set to allow the pilot to feel large lateral motion and side force cues. Pilot comments indicate that the motion cues were a significant improvement in comparison to fixed base simulation runs.

Instruments and controls- The VMS cockpit instrument panel design is shown in figure 4. Instruments included a radar altimeter, vertical speed indicator, attitude director indicator, airspeed meter, horizontal situation indicator, needle and ball, engine torque indicator, angle of attack indicator, "g" meter, and a clock. A set of panel lights gave targeting and weapon information and a panel-mounted CRT displayed the tactical situation. The function of both of these systems is discussed later in this report.

In the stowed position, and therefore not visible in figure 3 ,is a head-up display (HUD) which provided the information shown in figure 5. The HUD design was similar to that used in the experiment described in reference 9. This display was by far the primary source of flight information, as the pilot's vision was almost constantly directed outside the cockpit. The HUD weapon sighting was aligned daily to be certain that it corresponded to the firing logic, lights, and tones. Pilot utilization of the HUD information, particularly the velocity vector display, increased with experience.

The collective, cyclic, and directional controls were of a typical helicopter design. The force-feel characteristics of the cyclic stick and pedals were provided by an electro-hydraulic unit with adjustable breakout, static gradient, and viscous damping. These settings and the control travels are shown in table 11.

A drawing of the cyclic stick grip is shown in figure 6. The index finger trigger switch allowed the pilot to stop the simulation run at any time and return the motion and visual systems to the initial conditions. The lower thumb switch was the weapon firing control; the upper thumb switch would remove the stick force gradient if depressed. The evaluation pilots deemed initial stick gradients and dampings to be too large which lead them to fly the task with the upper thumb switch depressed. This caused a delay in reacting to firing opportunities. The problem ended when the stick forces were reduced to the values indicated in table 11.

CGI Visual System- The CGI data base (fig. 7) consisted of a detailed modeled area of approximately 9 km^2. The terrain included pyramid-type hills measuring up to 1000 ft in height, individual trees, and buildings. Solid "tree blocks" 30-50 ft in height were arranged with four clearings inside. The clearings were four-sided, measuring approximately 600 to 800 ft on a side. To increase visual cues, "postage stamp"-type dark squares were drawn on the hillsides, allowing the pilots better judgment of their height above the terrain than they would have had with monochromatic hillsides. The ground plane was a dusty brown color while the hills were various shades of green with sun vector shadowing. There was no ground texturing. A two-dimensional mountain range surrounded the detailed modeled area in a square pattern, 10 km on a side. In between the high detail area and this range was a flat ground plane. Both aircraft were free to fly anywhere in the data base.

The need for two independently piloted aircraft presented unique CGI requirements. The Singer-Link Digital Image Generator (DIG) normally provides the VMS pilot with four out-of-the-cockpit "windows" of CGI scenery. Since the DIG system has a capacity of four windows only, a two pilot system must split the four available windows between the two cockpits. For this simulation, a new DIG software program was developed to allow multiple eyepoints to be maneuvered about the data base. Three CGI windows were assigned to the eyepoint of the blue aircraft in the VMS cab, and one window was assigned to the other eyepoint at the red aircraft station. The fields-of-view that resulted are compared with that of a UH-60 Blackhawk in figure 8.

The pictorial presentation of the blue helicopter was that of a UH-60 Blackhawk while the red aircraft was represented as an MI-24 Hind (figs. 9 and 10). Both aircraft were depicted with rotating main rotor blades. Note that these were visual representations only; the math models producing the two aircrafts' flight characteristics are described later in this report. Occulting of the two images as they were obstructed by buildings, trees, or terrain occurred as it would normally in actual flight.

Special features of the new CGI database included a flash in each aircraft's CGI screen when a successful shot from the blue aircraft was fired. Visibility, though variable, was always set at clear daylight conditions for this experiment. Flightpaths of the red or blue helicopter were able to be recorded and then played back as a separate target during a simulation run. Thus, three aircraft, one preprogrammed and the other two piloted, could maneuver about the data base.

Head Up and Panel Mounted Displays- To compensate for the restricted field-of-view of the CGI visual system for air combat, a CRT panel-mounted display (PMD) for the blue aircraft cab and a similar HUD for the red aircraft were designed. The displays gave information as to the relative range, altitude, bearing, and heading of the opponent aircraft to each respective pilot in the pilot's own reference system. This information was displayed only if a clear line-of-sight existed between the two aircraft. A continuous scoring readout was also presented on each display.

Figure 11 shows a sample diagram of the information on the red aircraft HUD and blue aircraft PMD. Interpreting the diagram as the red aircraft HUD, the sample shows the blue aircraft in the seven o'clock position and heading directly at the red ship. Range is 1567 ft, and the large arrow and digits above it indicate that blue altitude is 222 ft greater than red. A short or medium length arrow would appear if blue was below red or at approximately the same altitude respectively. The scales at the upper left and right indicate each aircraft's probability of survival (PSR, PSB), starting at 100% and decreasing as shots were scored and the run progressed. The lower two scales appeared on the red aircraft HUD only and indicate red altitude and airspeed in analog and digital form.

The line of sight determination was calculated as follows. The coordinates of every hill and tree block vertex were stored in the mainframe computer memory. Planar surfaces were defined by grouping appropriate vertex sets. An algorithm was developed to determine if the line segment connecting the two aircraft intersected any of the planes. If an intersection was found, the line-of-sight was not clear, and the target information would not be displayed.

The blue aircraft PMD provided the evaluation pilots aid in initial acquisition during free engagements and they learned to use the display with quick glances whenever contact with the red aircraft was lost during tail chase maneuvers. One pilot commented that the PMD functioned similarly to an APR-39 missile warning radar system. The green light indicating a clear line-of-sight would alert the pilot to a threat presence and then a look at the PMD would give the location of the threat. A minor problem occurred due to the fact that the range circles on the display were spaced at 1 km intervals. As a result, the target arrow would overlay the center cross when the aircraft were at close range; the target's relative position would then become difficult to determine quickly. A solution to this problem would be to increase the range spacing, but then maximum detection range would be reduced. Some compromise however would be beneficial.

Red aircraft station- The red aircraft pilot operated the aircraft from a station set up in the VMS control room (fig. 12). Aircraft controls were a three axis joystick for roll, pitch, and yaw inputs and a potentiometer knob for collective control. A single window CGI picture was displayed on a 25-in. color monitor incorporating the field-of-view as shown in figure 13. The HUD discussed previously was projected on a beam-splitter system in front of the CGI monitor. A set of green, blue, and red panel lights duplicated the light display information in the VMS cab.

4.2 Firing Logic and Scoring

For simplicity, a fixed forward-firing weapon was modeled. It was assumed that if one aircraft could successfully track the other within certain range, pitch-off, and angle-off constraints for a representative time, then a probability of kill (PK) could be associated with that track. Pitch-off and angle-off are defined as the angles between an aircraft's body axis coordinates and an opponent aircraft in pitch and azimuth, respectively. These constraints describe a truncated cone as depicted in figure 1. Although the parameters were varied, the cone size was nominally set to ±2° in pitch and azimuth, and the optimum range was between 500 and 750 ft. These conditions had to be held for two continuous seconds to score a shot with PK = 0.10. A series of panel lights and headset tones alerted the pilot to the tactical situation and to when he was able to fire. When a successful shot was scored, the CGI displays flashed white for approximately 60 msec. A flow chart depicting the timer, light, and tone sequence for blue weapon firing is shown in figure 14.

Since the primary task of this experiment was tracking, measurements were set up to record and display to the blue pilot the relative success of his maneuvering. An "optimum" tail chase position was defined as a 30° body-axis cone projecting from the red aircraft as shown in figure 15. The cone is biased downward somewhat to reflect the advantage of being in the opponent's "blind spot." A maximum range of 1200 ft was also defined outside of which the opponent was assumed to have a turning advantage. If the blue aircraft strayed outside of these constraints for longer than five seconds, a probability of kill of 0.05 was charged to that event. During low level engagements, an altitude limit of 300 ft maximum was set in order to avoid ground-based defenses. If the blue aircraft exceeded this limit for longer than 13 sec, a probability of kill of 0.10 was charged.

For offensive maneuvers, the red aircraft was given a weapons cone identical to that of the blue aircraft. Red, however, did not need to depress a switch to fire a shot. If blue was held within the firing parameters for the required time, a shot was automatically scored with PK = 0.10. Whenever the blue aircraft was within the weapon parameters of the red aircraft during offensive engagements, or whenever blue strayed outside of the defined tail-chase position during tail-chase scenarios, a red light would be displayed on both the red and blue instrument panels. One second before a shot was to be fired, the light would begin to flash. A tone corresponding to the red light of a different pitch than the tone for the blue light was found to be confusing and not useful.

Shots were scored using a cumulative probability of survival model similar to that developed in reference 10. The PK values associated with successful shots or timer expirations were subjectively determined and do not necessarily represent actual PK values. With this model,

$$PSR(t + 1) = PSR(t) - (PSB)(PSR)(PKBA)$$

$$PSB(t + 1) = PSB(t) - (PSR)(PSB)(PKRA + PKRB + PKRC + PKRD)$$

where

PKXX = 0 if the scoring cases are not met

and

PKBA = 0.10 for a successful blue shot

PKRA = 0.10 for a successful red shot

PKRB = 0.05 if tail cone constraint timer exceeded

PKRC = 0.05 if range constraint timer exceeded

PKRD = 0.10 if maximum altitude timer exceeded

Using this model, cumulative probabilities of survival could be computed as an engagement progressed rather than having engagements terminated whenever a successful shot was fired. The engagements would terminate, however, if either aircraft reached a survival probability of 0.2. The current survival probabilities (PSR, PSB) were displayed to each pilot on the head up and panel mounted displays as described earlier.

4.3 Task

The majority of simulation runs were started with the blue aircraft already in a tail-chase position approximately 1000 ft behind the red aircraft. The blue pilot's task was to close to weapons range and maintain a proper tail-chase position as defined in the Firing Logic and Scoring section. The red aircraft was flown at various levels of aggressiveness from gentle pitches and rolls to much harder pitches, rolls, accelerations, and decelerations. Initial altitude was also varied from low level to 2000 ft.

Some engagements were staged in which the two aircraft were placed in positions in the data base unknown to each other. Each pilot was assigned a mission to fly to another designated point. During that transit, the aircraft would encounter each other, and air combat maneuvering would ensue. These free engagements resulted in the most aggressive maneuvering of the entire simulation. Structuring the task in this way also added to the pilot workload by forcing him to think tactically and organize his maneuver strategy accordingly. The free engagement was a more realistic (although less measurable) scenario than the tail chase since both aircraft were maneuvering offensively. A timer limited the length of each run from 90 to 120 sec for tail chase scenarios and to 4 to 5 min for free engagements.

4.4 Data Acquisition

Data taken for each simulated engagement were of four forms. Strip chart recorders kept track of 42 variables including control movements, airspeed, altitude, rate-of-climb, torque, and pitch, roll, and yaw angles and rates for each aircraft. Tracking information such as relative range, angle off, pitch off, timer histories

for each scoring case, and cumulative survival probabilities were also recorded on strip charts. An initial condition printout recorded the trim state of the blue aircraft and all design constraints, SCAS and control system settings. A final condition printout calculated the final survival probability of each aircraft and the total number of blue and red shots fired. (Each time a red scoring timer was exceeded a "shot" was fired.) Brief pilot comments were recorded on tape following each run and a Cooper-Harper handling qualities rating (fig. 16) was assigned for each configuration. Videotapes recording the blue center window CGI scene and head up display were also taken for most of the engagements.

5. RESULTS

The most significant results of the entire experiment were pilot comments regarding the high degree of realism of individual simulated encounters and of the overall simulation design. Both final evaluation pilots are instructors at the U.S. Navy Test Pilot School, Patuxent River, MD, and have significant helicopter, simulator, and evasive maneuvering experience (table 12). Following one encounter, pilot B commented:

> You have completely ruined me now. I am flying this mission the way I would a real EVM [evasive maneuvering] engagement. I was flying off the cues that I perceived and off the relative motion of the target aircraft. Even when I was above him in a hover, in a pedal turn, I've adapted enough now that I had him in the center of the right console window, maybe 20° down and was doing pedal turns keeping him there. I really flew that one the way I flew the ones at Patuxent River in relationship to the other aircraft, disregarding the ground. I never looked at my altimeter one time and I am now assimilating enough cues so I'm flying [the simulator] the way it is flown in the aircraft.

5.1 Angles and Rates

The chart in figure 17 is presented as a summary of the degree of maneuvering involved in the air combat task. The blue aircraft data are taken from 57 aggressive target maneuvering runs at low-level and clear-air altitudes. (Minimal differences were found between low-level and clear-air maximum rates and angles and the data are presented in combined form. However, the overall aggressiveness of the low level engagements seemed greater, although this is a subjective judgment.) Maximum roll rates between 25° and 55°/sec were most common. Maximum achieved values were an 84°/sec roll rate and 100° roll angle. These data lie somewhere between the 40°/sec maximum rate set for an OH-58 and the 60-100°/sec rates reported in reference 11 for the UH-60 and S-76 during ACM flight tests. The target aircraft was somewhat less agile and had a maximum achievable roll rate of just over 40°/sec. Red's maneuvering capability, therefore, was in the class of a teetering rotor system type aircraft in the roll axis.

Because the math models for each aircraft were not power limited, the aircraft could be accelerated to speeds in excess of 200 knots. This capability, however, was not used. The highest speed ever attained was approximately 160 knots, and this was a rare occurrence. Figure 17 shows the maximum speeds used to be centered around

108 knots. These speeds seemed to result because there the math models handled best rather than because of any specific speed requirement. That is, if the math models were most maneuverable at 80 knots, it is believed that the engagement airspeeds would have been lower.

5.2 Effects of Altitude

Pilot comments on the effect of altitude were as follows:

> Flight below 200 ft appeared to ease the performance of air combat tasks in some cases. This perception may have been the result of somewhat better perspective of altitude and attitude variations at the lower altitudes. Although the terrain afforded occasional opportunities for masking, once the engagement was initiated, the maneuvering was much more predictable in that the target aircraft became much more channelized. Additionally, the engagements at altitudes below 200 ft tended to be less in the vertical plane than those at higher altitudes. The exact differences in desirable flying qualities for engagements at low altitude compared with those at high altitude cannot be readily identified. Further testing is warranted in this area to identify the optimum flying qualities for air combat at low altitude.

In some instances, however, the maneuvering was more difficult at low altitude. On one occasion, as pilot B was tracking the target successfully, he saw the target pass a tree which he (pilot B) was going to have to avoid. Because he was flying a configuration with good handling qualities, he was able to press the attack until the timer was satisfied, fire a shot, and then avoid the tree at the last moment. Again, because the configuration was favorable, he was quickly able to reestablish a successful track. Clearly, this sort of problem does not occur at higher altitudes, and there the need for such agile and precise responses may not be strong. Handling quality requirements may, therefore, be different for low-level ACM. As pilot A noted, the maneuvering can become "channelized" if the target flies through a valley with terrain on both sides. In general, though, the requirements for low-level maneuvering seem to be more stringent than for clear-air combat. More data are needed, however, before these conclusions can be quantified and proven.

5.3 SCAS and Hub Configuration

As seen in figure 18, the effect of SCAS type was very noticeable while a change in modeled hub type seemed to have little effect. Data presented in the figure are averaged from all aggressive target maneuvering engagements (clear-air and low-level, tail chase, and free engagements). Individual pilot ratings are presented in table 13. A minimum of 8 to a maximum of 19 engagements were totaled for each listed combination of configuration and pilot. The attitude command system was rated from 1 to 2-1/2 rating points better on the average than the rate command system. For the high gain tracking task, tight control is required to keep the pipper sight on the target. The attitude command system allows the pilot to roll and pitch the aircraft to a desired angle with a single control movement. A rate command system requires two control movements to establish the same angle. During large amplitude maneuvering, however, some of the qualities of the rate system were desired. Larger angles could be commanded with smaller control inputs than with the attitude SCAS. In

general then, for the tight tracking task, an attitude command SCAS had advantages and whenever that track was lost or when maneuvering to attain a track, a rate command SCAS may be desirable.

One pilot's comments highlighted this observation:

> As far as the configuration is concerned, it is certainly a degradation over the attitude command system in terms of being able to nail an attitude and use it, but in terms of maneuverability, it is not nearly as restricted as the attitude command system seems to be. I notice I only use about plus or minus two inches of stick to get virtually any attitude I want out of the vehicle, whereas with the attitude command system, it seems that at some point, you want at least another twenty degrees of roll. Again, it is a tradeoff. I would be more inclined to take the attitude command system where I can at least get some shots off than I would to chase around all day with a system that is very maneuverable, but rather undependable in terms of being able to track with it.

As previously stated, a change in modeled hub type had little effect on pilot rating. The SCAS design was always the dominant variable and seemed to effectively mask any change in hub type. No restrictions owing to rotor system type were imposed upon the pilots. As reported in the experimental design section, the hub configuration changes were modeled in a general way. Any future simulation investigating these parameters would need to be more detailed.

Figure 19 presents a summary of the blue aircraft scoring and timer results. The total time the blue aircraft established a successful track on red (excluding momentary swings through the firing cone) was tabulated as a percentage of the total time of each run. This method was used over final probability of survival and shot-fired data due to the variability in run length. Only the NOE tail chase runs with nominal firing constraints were considered. Mean values for different configurations and pilot combinations are shown. The data seem to support pilot rating evaluations of the attitude command over the rate command SCAS and some evidence of performance differences due to hub type. The standard deviation for each of the points is on the order of their value, however, and the results cannot be considered conclusive. The sample size for the required combination of pilot/SCAS type/hub type/weapon parameters/initial relative position and initial altitude was unavoidably small. Sample sizes for the values presented range from a minimum of five to a maximum of twenty runs. The extremely variable nature of the task also led to somewhat variable results. A configuration with good handling qualities may have a low timer score on a particular engagement due to poor pilot technique, tactics, or more effective opponent maneuvering. A large number of runs with limited variability is required to establish conclusive results.

Typical pilot comments for the various configurations taken from the recordings taped following the completion of each run are summarized as follows:

CONFIGURATION A204: Most pronounced in A204 were very high levels of collective to pitch coupling which made the aircraft unpredictable in pitch control. Pitch bobbling was also preceived to be due to low longitudinal damping and sensitivity. Roll response was noted to be overly sensitive in comparison to the other rate control system in configuration B11.

CONFIGURATION B11: Although pitch coupling was not as pronounced as in configuration A204, it still remained the predominant deficiency. Some degree of roll to longitudinal cyclic or pitch rate coupling was noted. The roll axis control was acceptable. Some adverse yaw response to roll affected close-in tracking performance.

CONFIGURATION T05: Configuration T05 comments were highlighted by a perceived increae in pitch attitude stability over both B11 and A204. Pitch response was said to be much more predictable and roll response was good. The aircraft was noted to be not as maneuverable as the other configurations, however. (See section on rate vs attitude control.) The major deficiency in T05 was a tendency to PIO the directional axis when attempting to put the pipper on the target. When the aggressiveness with the pedals was reduced, the oscillations quickly damped out.

The tendency for deficiencies in pitch control to be noticed prior to directional control problems during the tracking task seemed to be a general one. That is, when pitch control handling qualities were improved, directional control problems became more apparent. This seems to indicate a relative importance of the two axes during the performance of the tracking task, or at least, the order in which the axes are controlled--pitch first and yaw second.

5.4 Effect of Weapon Parameters

A brief examination was made of the effect of extending the weapon range and constricting the firing constraint cone. The effect of opening the range from a maximum of 750 ft to 2000 ft while keeping a ±2° firing constraint cone was fairly dramatic. The tracking task was easier than during any other engagements even though the target maneuvering was still aggressive. Although simple geometry would indicate this is the case, it is still worthwhile to note the degree to which the task was affected. The handling qualities rating improved from a 4 to a 3, and the timer and scoring data show that the tracking was vastly improved. The target had only a 0.40 probablility of survival after the first minute of the engagement. Although this extended range is probably too long for a gun to be accurately fired, the launch constraints are applicable to missile systems. Thus, the relative ease of missile tracking compared to close-in gun tracking is highlighted.

5.5 Deficiencies

Simulation realism on the whole did not necessarily mean complete adequacy of individual parts. There were numerous deficiencies in the simulation, some of which are inherent to the simulator facilities and some which may be remedied for the future.

Simulation math model- Perhaps most significantly, the handling qualities of the basic aircraft math model needed improvement. In order to reduce the complexity of the experimental design, a standard version of the ARMCOP math model was used with configuration types from a previous NASA experiment on a different simulator facility. Current pilot ratings with the same configuration inputs never did reach the level of that experiment. Though the exact reasons are unclear, computer and simulator facility differences and model changes since the date of that experiment all probably contributed. Much time was spent trying to improve the basic model handling qualities before conducting the actual experiment. Pilot comments consistently referred to tracking problems in both the pitch and yaw axes. Control

sensitivities and dampings in these axes were varied to obtain an optimal setting. But because of the extremely variable and unpredictable nature of the task, and the effects of learning and configuration order, consistent pilot opinions were never quite reached.

The math model also did not adequately model aircraft maneuvering limitations. The engine was not power limited, and a perfect governor was assumed. Therefore, rotor rpm remained constant, and the pilot workload did not include monitoring rpm droop or torque limits. Mast bumping was not modeled for the teetering rotor, and the associated maneuvering limitations were not enforced. The pilots frequently commented that they felt they were using pedal inputs and sideslip to aid in target tracking to an unrealistic degree. Firing shots from such out-of-trim conditions offers little chance of precise aiming unless a sophisticated fire control computer is assumed.

CGI visual system- Also of important impact was the limited field-of-view available from the three CGI windows in the VMS cab. The field-of-view is compared to that of a UH-60 Blackhawk in figure 8, but even that is misleading since the Blackhawk has a reduced field-of-view when compared to the AH-1 Cobra or the AH-64 Apache. The important missing field is the upper center position which is needed not only when the target is at a higher altitude, but also during high G, close-in turns in order to keep the target in visual contact. The three-window display was surprisingly effective for most tracking situations though, and the PMD aided significantly during free engagements or when the target was lost. However, the limited field-of-view and the low resolution on the PMD at short ranges may have caused the lack of climbing, spiraling maneuvers reported during flight tests.

The pilots commented on the quality of the CGI visual system:

> Although the CGI was generally quite adequate for the purposes of this test, two deficiencies are notable. The first was that distances were not readily perceived, i.e., the cues required for depth perception were inadequate to enable some precision tasks such as hovering. This perception may be enhanced through the use of texture in the CGI. Second, the limited cues to rates of closure frequently caused both overshoots and widening of target distances without timely pilot responses. These delayed responses lengthened the time necessary to achieve the engagements or reduced the time that an engagement could be continued.

Motion system- Although the VMS has the largest vertical motion travel of any known aircraft flight simulator in the world, no simulator, however large, could exactly reproduce the motion cues experienced in air combat maneuvering. In order to stay within motion limits, the system response was scaled down as detailed earlier and motion cues were, therefore, lessened. This fact should be taken as an inherent deficiency of any such simulation. However, the pilots did rate the motion cues as being significant improvements over fixed base engagements which were conducted, and the motion cues were a valuable feature of the simulation.

Pilot comments were as follows:

> The quality of the simulator motion was generally considered extremely good. However, two observations may be made in relation to large amplitude maneuvers. It is unlikely that the design of

> the simulator considered the abrupt and large scale maneuvers prevalent during the evasive and pre-track maneuvering tasks. Therefore, the inconsistent motion cues, such as longitudinal bucking at highly banked (80°) turns, were not unexpected but do pose a limitation to the simulation of air combat. Additionally, the reduction of the motion gains in order to contain cab motion within the travel limitations also served to diminish the perceptibility of motion cues such as the detection of side force during more routine maneuvers.

At one point during the experiment, the motion system experienced technical problems. A number of fixed-base engagements were flown while the problems were being corrected. A sample of pilot comments regarding the differences between fixed base and motion simulations is as follows:

> The difference between being on motion and being off motion is still plaguing me a little bit. I'm much more mechanical in what I'm doing trying to think about what it would feel like and what it ought to be feeling like. Having to draw those cues out of the visual imagery is a little more difficult and I feel slightly more at a disadvantage.

> I can't say enough about the lack of motion cues. This simulator has better motion cues than any I have ever flown. To go from those cues one day to this [fixed-base flight] the next is a difficult transition to make quickly.

Handling qualities rating scale- The question of how to define the various configurations and how they performed as "inadequate," "adequate," or "satisfactory" was raised continually throughout the simulation. By its very nature, air-to-air maneuvering is an extremely complicated task with many factors affecting the end result. A number of those factors are outside the control of a particular pilot and often outside the realm of his aircraft. The opponent aircraft can dramatically change the ease of task performance by more gentle, more aggressive, or more clever maneuvering. Thus a pilot with an identical aircraft configuration for three different encounters may perform the tracking task extremely well or not at all. The rating assigned to that configuration may change due to what the pilot perceives as varying amounts of compensation to perform the same task. Also, one particular encounter could emphasize more lateral or more longitudinal control, or both, and particular aircraft deficiencies may be hidden or highlighted.

Of course, some of these problems affect all sorts of piloted simulations. What seems to be unique about the air-to-air task is that a fully realistic simulation requires unpredictability in the flightpath of the target vehicle so the pilot will not be able to anticipate his opponent's maneuvering and "cheat" in his tracking. This "cheating" would result in reduced aggressiveness by that aircraft and might allow the pilot to perform the tracking task without the constant and sometimes violent course corrections that are characteristic of air-to-air combat. On the other hand, any experimenter wishes to limit variability in order to establish conclusive results with a manageable number of test points. Because this was the initial simulation effort in this area, it was intended to investigate the subject in a broad fashion. Thus, as stated earlier, the only limit to target maneuvering variability was a general (but conscious) effort by the target pilot to be consistent in the target aircraft's level of aggressiveness.

The pilot ratings for each of the various configurations, therefore, had a tendency to vary significantly between encounters. Following discussions with the evaluation pilots, "inadequate," "adequate," and "satisfactory" handling qualities ratings were to be based on their experience from flight tests judging what is necessary to accomplish the task. It was left to their judgment to separate the effects of their own aircraft's handling qualities, target aggressiveness, and each aircraft's tactical strategy when giving a rating to a particular configuration. This was often not an easy judgment to make.

In the future, multiple rating scales specific to factors such as those mentioned above might be employed to adjust the overall rating. In addition, some reduction in the variability of the target maneuvering seems to be in order. A number of possibilities, such as a library of prerecorded flight paths, a computer controlled opponent, or variations of an open-loop analytical function describing a flightpath are currently being investigated.

6. CONCLUSIONS

The large number of experimental variables and the exploratory nature of the simulation tend to prohibit specific definitive conclusions from being set forth. However, some points can be stated with confidence. The simulator system design, facilities, and pilot tasks were all judged to be extremely useful tools for evaluating a wide variety of aspects of the helicopter air combat maneuvering problem. Engagement tactics and flight paths of both the red and blue aircraft were found to be representative of both flight test encounters and scenarios that military pilots would expect to see in actual combat. In short, a legitimate capability to perform realistic and meaningful simulations of low altitude helicopter air combat encounters has been developed and proven.

Other general conclusions can be drawn. Pilot comments, handling qualities ratings and scoring performance showed the characteristics of the attitude command SCAS to be superior during the tracking phase of the task, while the rate command system had characteristics desired for larger amplitude maneuvers. While this was only a limited examination, a control system which can combine the qualities of both systems is worthy of future investigation; for example, a transition from attitude to rate command system as a function of controller displacement may provide the desired blend of control response.

Low-level maneuvering in the presence of terrain features brought a high degree of realism to the simulation. The effect of the terrain seems to be an important one although the exact performance agility differences from clear-air maneuvering cannot be determined from the limited data taken. Certainly, maneuver strategies were affected and ground and obstacle avoidance were continuous pilot concerns. It seems imperative to include these terrain features in any high fidelity simulation of helicopter air combat. Quantification of their effect on handling qualities requirements will be an important focus of future studies.

Although only a simple examination of a change in weapon parameters was performed, the fact that any change has a substantial effect on the tracking task should be highlighted. The weapon system model will have a first-order effect on any encounter result, either actual or simulated. A more precise model or an examination of various weapon types should be included in future studies.

Future simulation experiments in helicopter air combat maneuvering could focus on any of the number of variables discussed here, or on others, such as auxiliary thrust configurations, an ABC or tilt rotor model, or multiple player encounters. Regardless of the variable examined, the experimental design will need to be tightly controlled in order to generate conclusive results about what has been found to be an extremely variable and complex subject.

APPENDIX

RED AIRCRAFT EQUATIONS OF MOTION

1. INTRODUCTION

Several criteria determined the selection of the equations of motion for the target (or red), aircraft for this simulation. Because of computer capacity limits, the model was required to be relatively simple. However, because the resultant motions of the red aircraft were to be presented visually to the pilot of the blue aircraft, the model had to exhibit helicopter-like dynamics, including realistic attitude-speed relationships so as to provide the proper cues to guide the blue pilot's maneuvers. No airspeed restrictions were applied to the engagements; therefore, the red aircraft model was required to be capable of realistic maneuvers at hover, low speeds, and in forward flight. Finally, because the red aircraft was to be flown from a pilot's station equipped with a limited field-of-view visual display and a simple joystick controller, the aircraft had to be relatively easy to fly. Specifically, in hover and low speed flight, a pitch and roll attitude command system is provided; an altitude rate command and yaw rate command system are provided in the vertical and directional axes, respectively. In forward flight, the pitch and roll axes are transformed into angular rate command systems while the directional axis provides an automatic turn coordination feature.

This discussion of the red aircraft mathematical model is divided into three sections: (1) pilot's control inputs, (2) rotational equations of motion, and (3) translational equations of motion. The computer mneumonics used in this description correspond to those used in the actual FORTRAN subroutine TMAN.

2. PILOT'S CONTROL INPUTS

The pilot's pitch, roll, yaw, and vertical control inputs from the joystick controller (PITCHT, ROLLT, YAWT, and DCT, respectively) are expressed in terms of percent of full scale. Limits of ±50% are imposed on each of the inputs and selectable deadbands (PDBT, RDBT, YDBT, and CDBT, respectively) are provided; these deadbands were set to ±2% for this experiment.

3. ROTATIONAL EQUATIONS OF MOTION

The equations of motion for the three rotational degrees of freedom provide a pitch and roll attitude command system and a yaw rate command system below an airspeed of 30 knots. Above 50 knots, a pitch and roll rate command system is provided while the yaw axis acts to maintain zero lateral acceleration (automatic turn coordination). The equations for body-axis roll, pitch, and yaw accelerations in rad/sec^2 are:

```
PBDT=ZLPT*ROLLDR+XLDAT*ROLLT+XLPHIT*PHITR
```

QBDT=ZMQT*PITCHDR+XMDET*PITCHT+MTHETT*(THETETR+TMDUM)

RBDT=XNVT*VBT+ZNRT*YAWDR+ZNPT*ROLLDR+XNPHIT*PHITR+XNDPT*YAWT

where

ROLLDR, PITCHDR, YAWDR = body-axis roll, pitch, and yaw rates, respectively (rad/sec)

PHITR, THETATR = roll and pitch Euler angles, respectively (rad)

TMDUM = correction for trim pitch attitude variations

= .000621*UBT (rad)

UBT, VBT = body-axis longitudinal and lateral velocity components, respectively (ft/sec)

ZLPT, ZMQT, ZNRT = roll, pitch, and yaw rate damping derivatives, respectively (1/sec)

XLDAT, XMDET, XNDPT = roll, pitch, and yaw control sensitivities, respectively (rad/sec^2/%)

XLPHIT, XMTHETT = roll and pitch attitude stability derivatives, respectively (1/sec^2)

and

XNVT (rad/ft-sec), ZNPT (1/sec), and XNPHIT (1/sec^2) help provide the automatic turn coordination feature

The nominal values of the stability derivatives were selected to provide the desired control responses throughout the airspeed envelope. Below 30 knots, a critically damped second-order response of pitch and roll rate to control input with a natural frequency of 2.0 rad/sec was provided; in the directional axis, a first-order yaw rate response with a 0.5 sec time constant was selected. Above 50 knots, a first-order response of pitch and roll rate to control input with a time constant of 0.36 sec was provided. Yaw control inputs resulted in a critically damped second-order response in sideslip with a natural frequency of 1.5 rad/sec. With no yaw control inputs, lateral acceleration was maintained at zero. Blending of these control responses occurred between 30 and 50 knots.

The rate damping derivatives remained constant for all airspeeds: ZLPT=-2.8, ZMQT=-2.8, and ZNRT=-2.0. The other stability derivatives were functions of airspeed (VEQT, knots) as follows:

	VEQT<30	30<VEQT<50	VEQT>50
XLPHIT	-4.0	VEQT/5.0-10.0	0.0
XMTHETT	-4.0	VEQT/5.0-10.0	0.0
XNVT	0.0	.00133*VEQT-.0399	1.33/VEQT
ZNPT	0.0	.019*VEQT-0.57	19.0/VEQT
XNPHIT	0.0	.038*VEQT-1.14	38.0/VEQT

The control sensitivities were selected to be: XLDAT=0.04, XMDET=0.02, and XNDPT=0.02.

Integration of the angular accelerations yield the body-axis angular rates in rad/sec (ROLLDR, PITCHDR, and YAWDR) and in deg/sec (ROLLD, PITCHD, and YAWD). Euler angular rates in deg/sec are then calculated using sines and cosines of PHITR and THETATR (SINPHI, COSPHI, SINTHET, COSTHT) as:

```
THETTD=PITCHD*COSPHI-YAWD*SINPHI

PSITD=(PITCHD*SINPHI+YAWD*COSPHI)/COSTHT

PHITD=ROLLD+PSITD*SINTHET
```

These angular rates are then integrated to obtain aircraft Euler angles in degrees (THETAT, PSIT, and PHIT) and radians (THETATR, PSITR, and PHITR). The sines and cosines of the Euler angles are then calculated, and the elements of the red aircraft earth axis-body axis transformation matrix are formed.

4. TRANSLATIONAL EQUATIONS OF MOTION

The equations which define the three translational degrees of freedom were selected to provide realistic speed-attitude relationships and to ensure an acceptable vertical response to control input. The equations for body-axis longitudinal, lateral, and vertical forces in pounds are as follows:

```
FTXT=TWAIT/G*(XRT+XUT*UBT)

FTYT=TWAIT/G*(YRT+YVT*VBT)

FTZT=TWAIT/G*(ZRT+ZWT*WBT+ZDCT*DCT)
```

where

TWAIT = target weight (lbs, nominally = 10,000)

G = acceleration due to gravity (32.2 ft/sec^2)

XRT,YRT,ZRT = longitudinal, lateral, and vertical reference accelerations, respectively (ft/sec^2)

XUT,YVT,ZWT = longitudinal, lateral, and vertical speed damping derivatives, respectively (1/sec)

WBT = body-axis vertical velocity component (ft/sec)

ZDCT = vertical control sensitivity ($ft/sec^2/\%$)

For this experiment, XRT and YRT were set to zero to yield zero hover trim values of pitch and roll attitude, respectively. ZWT was assigned a value of -1.0 to produce a first-order response in vertical velocity to a control input with a time constant of 1.0 sec; ZDCT was set to 1.5 to provide the desired control response

sensitivity. To trim the vertical force equation, ZRT was calculated in the initial conditions section to be equal to -ZWT*WBT-G*COSTHT. To achieve the desired speed-attitude relationships, XUT was set at a value of -0.02 and YVT was set to -0.1; these values yield an incremental trim pitch attitude change of -0.6° for each 10 knot increase in forward speed and approximately 3.0° of roll angle to achieve a 10 knot change in lateral velocity at hover. To simulate red aircraft g-limits, FTZT was limited to values no less than FZMIN and no greater than FZMAX, where FZMIN=ZNMIN*TWAIT and FZMAX=ZNMAX*TWAIT; for this experiment, ZNMIN was set to 0.5 g and ZNMAX to 2.5 g.

These body-axis forces are then transformed to the earth axis system (North, East, Down) to determine FNT, FET, and FDT using the transformation calculated in the rotational equations. Accelerations in this axis system (VNDT, VEDT, and VDDT) are calculated by multiplying the forces by G/TWAIT; TWAIT is added to FDT prior to this multiplication. Integration of the earth-axis accelerations yields the earth-referenced velocity components VNT, VET, and VDT. A transformation of these velocities back to the body axis is then required to calculate UBT, VBT, and WBT.

5. INITIAL CONDITIONS

Rather than using iterative techniques to achieve an initial trim state, the initial conditions of the model are calculated in closed-form. The initial control inputs are zeroed and the initial values of the angular rates are set to zero. Initial roll angle is set to zero while the initial value of aircraft heading (PSIT) is specified by the user. The trim pitch attitude is calculated by computing the arcsine of FTXT/TWAIT. The initial value of VEQT is specified by the researcher, and the resultant initial velocity components are specified as VNT=VEQT*COS(PSITR), VET=VEQT*SIN(PSITR), and VDT=0. The vertical force equation is trimmed as indicated in the preceding section.

6. CONCLUDING REMARKS

The six degree-of-freedom equations of motion of the red aircraft developed for the helicopter air combat experiment yield a model which is relatively easy to fly and yet exhibits (to an outside observer) all the major dynamic characteristics of a typical helicopter. The model exhibited mild transient abnormalities as the 30 and 50 knot stability derivative phasing speeds. The elimination of these transients was not investigated. Performance limits of specific rotorcraft can be imposed on the model through limits on the control inputs or by limiting the resultant translational or rotational accelerations appropriately.

REFERENCES

1. Anon.: Air-to-Air Combat Test Flight Test Plan (AACT II), Applied Technology Laboratory, U.S. Army Research and Technology Laboratories (AVSCOM), Fort Eustis, VA, Jun. 1983.

2. Anon.: Rotary Wing Air Combat Maneuvering Guide. Third Draft, 3/5 Cavalry, Fort Lewis, WA, and 2/17 Cavalry, Fort Campbell, KY, Aug. 1983.

3. Harris, T. M.; Wood, R. K.: Helicopter Effectiveness in Air-to-Air Combat. Flight Systems, Inc., FSI TR 79-73, Nov. 1979.

4. Falco, M.: Light Helicopter Air-to-Air Combat. Grumman Aerospace Corporation. RE-683, Apr. 1984.

5. Chen, R. T. N.; Talbot, P. D.; Gerdes, R. M.; and Dugan, D. C.: A Piloted Simulator Study on Augmentation Systems to Improve Helicopter Flying Qualities in Terrain Flight. NASA TM-78571, Mar. 1979.

6. Talbot, P. D.; Dugan, D. C.; Chen, R. T. N.; and Gerdes, R. M.: Effects of Rotor Parameter Variations on Handling Qualities of Unaugmented Helicopters in Simulated Terrain Flight. NASA TM-81190, Aug. 1980.

7. Talbot, P. D.; Tinling, B. E.; Decker, W. A.; and Chen, R. T. N.: A Mathematical Model of a Single Main Rotor Helicopter for Piloted Simulation. NASA TM-84281, Sept. 1982.

8. Jones, A. D.: Operations Manual: Vertical Motion Simulator (VMS) S.08. NASA TM-81180, May 1980.

9. Aiken, Edwin W.; Landis, Kenneth H.: An Assessment of Various Side-Stick Controller/Stability and Control Augmentation Systems for Night Nap-of-the-Earth Flight Using Piloted Simulation. Presented to the American Helicopter Society, Palo Alto, CA, Apr. 1982.

10. Hague, D. S.: An Introduction to Co-Kill Probability Estimation in the M-on-N Encounter, AIAA Paper 79-1729, AIAA Guidance and Control Meeting, Boulder, CO, Aug. 1979.

11. Lappos, N. D.: Insights Into Helicopter Air Combat Maneuverability. Presented at the 40th Annual Forum of the American Helicopter Society, Crystal City, VA, May 1984.

TABLE 1.- TEST CONFIGURATIONS

Configuration	γ	e	k_β ft-lb/rad	SCAS
A204[a]	3	0.05	97,780	Rate
B11[b]	9	.14	13,040	Rate
T05 T	6	0	0	Attitude
T05 A[b]	3	.05	97,780	Attitude
T05 H	9	.14	13,040	Attitude

[a]Ref. 6
[b]Ref. 7

TABLE 2.- GEOMETRIC CHARACTERISTICS OF BASELINE HELICOPTER CONFIGURATION

Weight, lb	8000
Main rotor	
x, z, ft	0.0, 6.57
rpm, rad/sec	33.0
Diameter, ft	44.0
Chord, ft	2.25
Number of blades	2
Solidity	0.0651
δ_3, deg	0.0
Horizontal tail	
x, z, ft	16.54, -1.27
Area, ft^2	14.6
Vertical tail	
x, z, ft	25.08, 1.07
Area, ft^2	18.6
Tail rotor	
x, z, ft	26.73, 3.93
rpm, rad/sec	173.4
Diameter, ft	10.0
Control throws	
Pitch/roll/yaw, in.	±6/±6/±3.25
Collective, in.	10

TABLE 3.- INPUT DECOUPLING GAINS

	Units	Gains	Value	(V in knots)
Configuration A204	in./in.	Δ_{ES}/δ_{CS}	0	0
	in./in.	Δ_{RP}/δ_{CS}	0	0
Configuration T05H, T, A	in./in.	Δ_{ES}/δ_{CS}	0	(V = 0)
			-0.40	(V = 60)
			-.80	(V = 120)
	in./in.	Δ_{RP}/δ_{CS}	-.447	(V = 0)
			-.208	(V = 60)
			-.214	(V = 120)
Configuration B11	in./in.	Δ_{ES}/δ_{CS}	0.0	(V = 0)
			-0.4	(V = 60)
			-.8	(V = 120)
	in./in.	Δ_{RP}/δ_{CS}	-.447	(V = 0)
			-.196	(V = 60)
			-.133	(V = 120)

TABLE 4.- FEEDBACK AND GEARING GAINS

	Units	Gains	Value
Configuration A204	in./in.	Δ_{ES}/δ_{ES}	1.25
	in./in.	Δ_{AS}/δ_{AS}	1.00
	in./in.	Δ_{CS}/δ_{CS}	1.00
	in./in.	Δ_{RP}/δ_{RP}	1.00
	in./ft/sec	Δ_{ES}/u	-.00927
	in./rad/sec	Δ_{AS}/p	0
	in./ft/sec	Δ_{CS}	0
	in./ft/sec	Δ_{RP}/u	0
	in./rad/sec	Δ_{RP}/r	-.27
Configuration T05T, A, H	in./in.	Δ_{ES}/δ_{ES}	2.00
	in./in.	Δ_{AS}/δ_{AS}	1.50
	in./in.	Δ_{CS}/δ_{CS}	1.00
	in./in.	Δ_{RP}/δ_{RP}	1.00
	in./ft/sec	Δ_{ES}/u	-.0102
	in./rad	$\Delta_{ES}/\Delta\theta$	-.0713
	in./rad/sec	Δ_{ES}/q	-.0562
	in./rad	$\Delta_{AS}/\Delta\phi$	-2.17
	in./rad/sec	Δ_{AS}/p	-.505
	in./ft/sec	Δ_{CS}/w	0
	in./ft/sec	Δ_{RP}/v	0.020
	in./rad/sec	Δ_{RP}/r	-.735
Configuration B11	in./in.	Δ_{ES}/δ_{ES}	1.25
	in./in.	Δ_{AS}/δ_{AS}	1.50
	in./in.	Δ_{CS}/δ_{CS}	1.00
	in./in.	Δ_{RP}/δ_{RP}	1.00
	in./ft/sec	Δ_{ES}/u	-.00986
	in./rad/sec	Δ_{ES}/q	0.0
	in./ft/sec	Δ_{AS}/v	0.0
	in./rad/sec	Δ_{AS}/p	0.0
	in./ft/sec	δ_{RP}/u	.00414
	in./ft/sec	Δ_{RP}/v	.02
	in./rad/sec	Δ_{RP}/r	-.735

TABLE 5.- STABILITY AND CONTROL DERIVATIVES FOR CONFIGURATION A204 (60 knots)

The F matrix is							
u	w	q	θ	v	p	ϕ	r
-0.84280E-02	-0.33966E-02	0.73811E 01	-0.32193E 02	-0.21792E-01	-0.71724E 00	0.00000E 00	0.24127E 02
-.51476E-01	-.74560E 00	.99601E 02	.65632E 00	-.23411E-01	-.25462E 02	.00000E 00	-.27386E-01
.55685E-03	.12128E-02	-.55096E 01	.00000E 00	-.11143E-02	.29130E 00	.00000E 00	-.82209E-02
.00000E 00	.00000E 00	.10000E 01	.00000E 00	.00000E 00	.00000E 00	.00000E 00	.00000E-00
-.95117E-02	-.52387E-02	-.30607E 00	.00000E 00	-.10112E 00	-.76659E 01	.32193E 02	-.97003E 02
-.12121E-01	-.17050E-01	-.63104E 00	.00000E 00	-.44822E-01	-.25925E 02	.00000E 00	.16847E-00
.00000E 00	.00000E 00	.00000E 00	.00000E 00	.00000E 00	.10000E 01	.00000E 00	-.20387E-01
-.25895E-02	-.12337E-01	.14223E 00	.00000E 00	.26851E-01	-.23934E 01	.00000E 00	-.12397E 01
The G matrix is							
		δe	δa	δc	δp		
		-0.14966E 01	0.26852E 00	0.72015E-01	0.10871E-03		
		-.27994E 01	-.81973E 01	.13782E 01	.10220E-01		
		.12794E 01	-.18171E 00	-.21713E-01	.97761E-02		
		.00000E 00	.00000E 00	.00000E 00	.00000E 00		
		.43478E-01	.88942E-01	.11977E 01	-.13054E 01		
		-.36148E-01	-.41774E 00	.48571E 01	-.22256E 00		
		.00000E 00	.00000E 00	.00000E 00	.00000E 00		
		-.46209E-01	-.28374E-01	.43820E 00	.78697E 00		

TABLE 6.- STABILITY AND CONTROL DERIVATIVES FOR CONFIGURATION T05T (60 knots)

The F matrix is

u	w	q	θ	v	p	ϕ	r
-0.55392E-03	0.86589E-02	0.57051E 01	-0.32200E 02	-0.89735E-02	-0.13134E 01	0.00000E 00	0.90788E 01
-.24700E 01	-.74374E 00	.11101E 03	-.14760E 00	-.23002E-01	-.10387E 02	.00000E 00	-.28107E-01
-.79456E-03	-.69205E-02	-.93007E 00	.00000E 00	.70236E-03	.16791E 00	.00000E 00	-.10679E-01
.00000E 00	.00000E 00	.10000E 01	.00000E 00	.00000E 00	.00000E 00	.00000E 00	.00000E 00
.10368E-02	-.12738E-01	-.10038E 01	.00000E 00	-.11664E 00	-.22928E 01	.32200E 02	-.98938E 02
.76809E-03	-.97419E-02	-.62390E 00	.00000E 00	-.93934E-02	-.16845E 01	.00000E 00	.35750E 00
.00000E 00	.00000E 00	.00000E 00	.00000E 00	.00000E 00	.10000E 01	.00000E 00	.45840E-02
-.27808E-02	-.98736E-02	.19139E-01	.00000E 00	.46252E-01	-.23712E 00	.00000E 00	-.15899E 01

The G matrix is

		δe	δa	δc	δp		
		-0.14270E 01	0.22982E 00	-0.35106E-02	.13138E-01		
		-.33670E 01	-.83860E 01	.19150E 00	.89619E-02		
		.19016E 00	-.10389E-01	-.23270E-04	.66092E-02		
		.00000E 00	.00000E 00	.00000E 00	.00000E 00		
		-.68076E-01	.14600E 00	.94383E 00	-.13075E 01		
		-.56545E-01	.29928E-01	.58911E 00	-.22007E 00		
		.00000E 00	.00000E 00	.00000E 00	.00000E 00		
		-.44283E-01	.59902E-02	.53464E-01	.78810E 00		

TABLE 7.- STABILITY AND CONTROL DERIVATIVES FOR CONFIGURATION T05A (60 knots)

The F matrix is

u	w	q	θ	v	p	ϕ	r
-0.17796E-02	-0.35969E-02	0.11840E 02	-0.32193E 02	-0.19374E-01	-0.73761E 00	0.00000E 00	0.24184E 02
-.39039E-01	-.74595E 00	.10792E 03	.65542E 00	-.18537E-01	-.25911E 02	.00000E 00	-.32251E-01
-.51492E-02	.13857E-02	-.93190E 01	.00000E 00	-.29935E-02	.29746E 00	.00000E 00	-.12766E-01
.00000E 00	.00000E 00	.10000E 01	.00000E 00	.00000E 00	.00000E 00	.00000E 00	.00000E 00
-.65944E-02	-.51633E-02	-.43521E 00	.00000E 00	-.12777E 00	-.00081E 01	.32193E 02	-.96381E 02
-.11427E-01	-.17043E-01	-.52290E 00	.00000E 00	-.49307E-01	-.27307E 02	.00000E 00	.27186E 00
.00000E 00	.00000E 00	.00000E 00	.00000E 00	.00000E 00	.10000E 01	.00000E 00	-.20359E-01
-.42607E-02	-.12383E-01	.27981E 00	.00000E 00	.42940E-01	-.25182E 01	.00000E 00	-.16056E 01

The G matrix is

		δe	δa	δc	δp		
		-0.15873E 01	0.10701E 00	0.60845E-01	-0.12160E-03		
		-.29680E 01	-.85003E 01	.11643E 01	.10220E-01		
		.13568E 01	-.43604E-01	-.18346E-01	.97784E-01		
		.00000E 00	.00000E 00	.00000E 00	.00000E 00		
		.46155E-01	.93566E-01	.10117E 01	-.13053E 01		
		-.38332E-01	-.42178E 00	.41023E 01	-.22256E 00		
		.00000E 00	.00000E 00	.00000E 00	.00000E 00		
		-.40991E 01	-.33309E-01	.37010E 00	.78696E 00		

TABLE 8.- STABILITY AND CONTROL DERIVATIVES FOR CONFIGURATION T05H (60 knots)

The F matrix is

u	w	q	θ	v	p	ϕ	r
-0.35799E-02	-0.75448E-02	0.85902E 01	-0.32195E 02	-0.23103E-01	-0.74153E 00	0.00000E 00	0.19385E 02
-.38143E-01	-.73948E 00	.10874E 03	.58383E 00	-.20754E-01	-.21293E 02	.00000E 00	-.31890E-01
-.29738E-02	-.36736E-03	-.53876E 01	.00000E 00	-.18653E-02	.13692E 01	.00000E 00	-.21167E-01
.00000E 00	.00000E 00	.10000E 01	.00000E 00	.00000E 00	.00000E 00	.00000E 00	.00000E 00
-.45622E-02	.25118E-02	-.53368E 00	.00000E 00	-.12953E 00	-.50374E 01	.32195E 02	-.97415E 02
-.59021E-02	-.25167E-02	-.59394E 01	.00000E 00	-.44266E-01	-.11948E 02	.00000E 00	.38929E 00
.00000E 00	.00000E 00	.00000E 00	.00000E 00	.00000E 00	.10000E 01	.00000E 00	-.18134E-01
-.38210E-02	-.11685E-01	-.36045E 00	.00000E 00	.43469E-01	-.10091E 01	.00000E 00	-.15950E 01

The G matrix is

		δe	δa	δc	δp		
		-0.14613E 01	0.61660E-01	0.42730E-01	-0.22749E-02		
		-.28325E 01	-.86030E 01	.10177E 01	.10691E-01		
		.10654E 01	-.22290E-01	-.17984E-02	.10329E-01		
		.00000E 00	.00000E 00	.00000E 00	.00000E 00		
		.43028E-01	.15475E 00	.91062E 00	-.13054E 01		
		-.81851E-01	-.17667E 00	.32054E 01	-.22291E 00		
		.00000E 00	.00000E 00	.00000E 00	.00000E 00		
		-.50674E-01	-.10848E-01	.28141E 00	.78701E 00		

TABLE 9.- STABILITY AND CONTROL DERIVATIVES FOR CONFIGURATION B11 (60 knots)

The F matrix is							
u	w	q	θ	v	p	ϕ	r
-0.10204E-02	-0.75823E-02	0.46857E 01	-0.32193E 02	-0.22721E-01	-0.72710E 00	0.00000E 00	0.26298E 02
-.33143E-01	-.73950E 00	.99191E 02	.65909E 00	-.20078E-01	-.27864E 02	.00000E 00	-.31890E-01
-.48034E-02	-.34395E-03	-.23966E 01	.00000E 00	-.21476E-02	.13687E 01	.00000E 00	-.21165E-01
.00000E 00	.00000E 00	.10000E 01	.00000E 00	.00000E 00	.00000E 00	.00000E 00	.00000E 00
-.10045E-01	.25116E-02	-.41284E 00	.00000E 00	-.12955E 00	-.49293E 01	.32193E 02	-.95815E 02
-.66767E-02	-.25241E-02	-.61691E 01	.00000E 00	-.44253E-01	-.10870E 02	.00000E 00	.38933E 00
.00000E 00	.00000E 00	.00000E 00	.00000E 00	.00000E 00	.10000E 01	.00000E 00	-.20473E-01
-.47117E-03	-.11693E-01	-.50272E 00	.00000E 00	.43482E-01	-.91439E 00	.00000E 00	-.15950E 01
The G matrix is							
		δe	δa	δc	δp		
		-0.10578E 01	0.10781E 00	0.57203E-01	-0.22829E-02		
		-.20490E 01	-.85141E 01	.13622E 01	.10691E-01		
		.77104E 00	-.55932E-01	-.24008E-02	.10329E-01		
		.00000E 00	.00000E 00	.00000E 00	.00000E 00		
		.31136E-01	.15334E 00	.12192E 01	-.13054E 01		
		-.59249E-01	-.17415E 00	.42907E 01	-.22291E 00		
		.00000E 00	.00000E 00	.00000E 00	.00000E 00		
		-.36693E-01	-.92407E-02	.37670E 00	.78701E 00		

TABLE 10.- MOTION SYSTEM PARAMETERS

(Cockpit oriented for large lateral travel)		
Description	Computer mnemonic	Value
High frequency motion gains	GXF	0
	GYF	.5
	GZF	.4
	GPF	.4
	GQF	.4
	GRF	.4
Washout filter frequency (rad/sec)	OMEGXF	1.0
	OMEGYF	.7
	OMEGZF	.8
	OMEGPF	.8
	OMEGQF	.6
	OMEGRF	.6

TABLE 11.- CONTROL TRAVELS AND FORCE GRADIENTS

Control	Travel, in.	Breakout, lb approximate	Gradient, lb/in.
Collective	10.0	0.50	0
Pedals	±3.25	2.00	2.00
Longitudinal cyclic	±6.00	1.00	.67
Lateral cyclic	±6.00	1.00	1.00

TABLE 12.- PILOT EXPERIENCE

	Pilot	
	A	B
Total hours	3350	5700
Total rotary wing, hr	3100	4700
Primary A/C	CH-46, AH-1, UH-1	AH-1, UH-1, UH-60
Other A/C	OH-58, BO-105, Bell 412 CH-53, others	OH-58, CH-47, OV-1 CH-46, ABC, others
Evasive maneuvering time, hr	30	30
Simulator time, hr	50	300

TABLE 13.- INDIVIDUAL PILOT RATINGS

Pilot A				
Run number/pilot rating				
T05H	T05A	T05T	A209	B11
10/4	45/6	91/4	2/5	49/8
11/6	46/5	92/4	3/4	50/7
12/5	47/5	93/4	17/6	51/8
13/3	73/5	94/4	41/9	52/7
56/7	74/5	95/4	71/7	53/7
151/4	75/4	96/4	72/6	54/7
152/3	78/4	97/4	101/7	55/7
153/7	79/4	98/4	102/7	77/6
154/7	80/4	99/4		103/6
155/5	81/5	100/4		
156/4	82/6			
157/4	86/3.5			
158/3.5				
159/4				
160/4				
161/3				
162/3				
164/5				
165/7				
Pilot B				
21/6	5/4		18/3	26/6
22/3	7/6		20/4	27/6
23/4	21/6		34/8	28/6
32/3	22/3		36/6	29/7
33/3	23/4		37/7	30/2
110/5	25/4		58/5	31/2
116/4	61/4		59/7	38/7
141/6	62/3		60/5	106/6
142/3	63/3		61/4	107/6
143/6.5	64/4			108/4
144/3	65/4			109/7
146/4	66/4			117/6
				118/4
				148/6

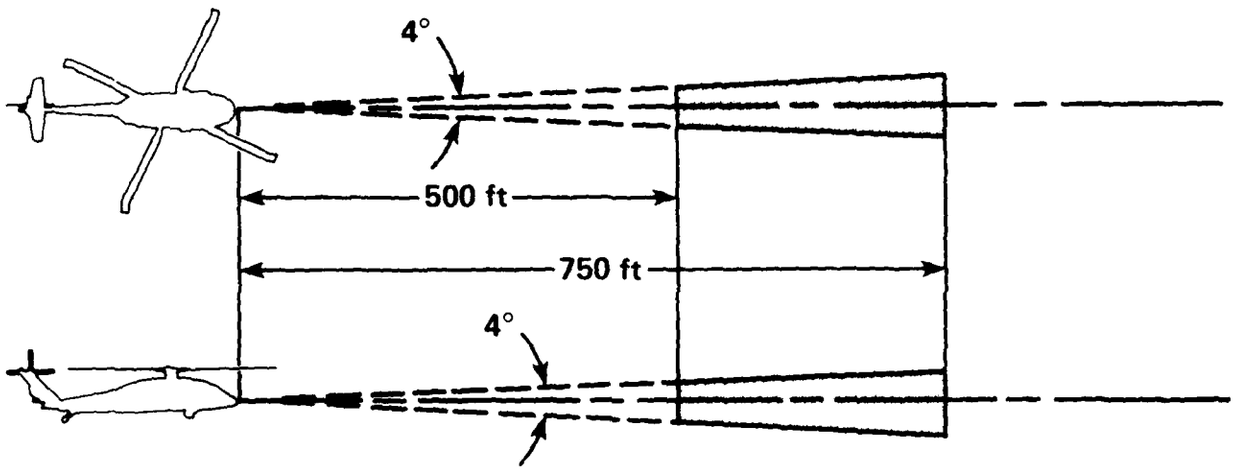

Figure 1.- Simulated weapon envelope.

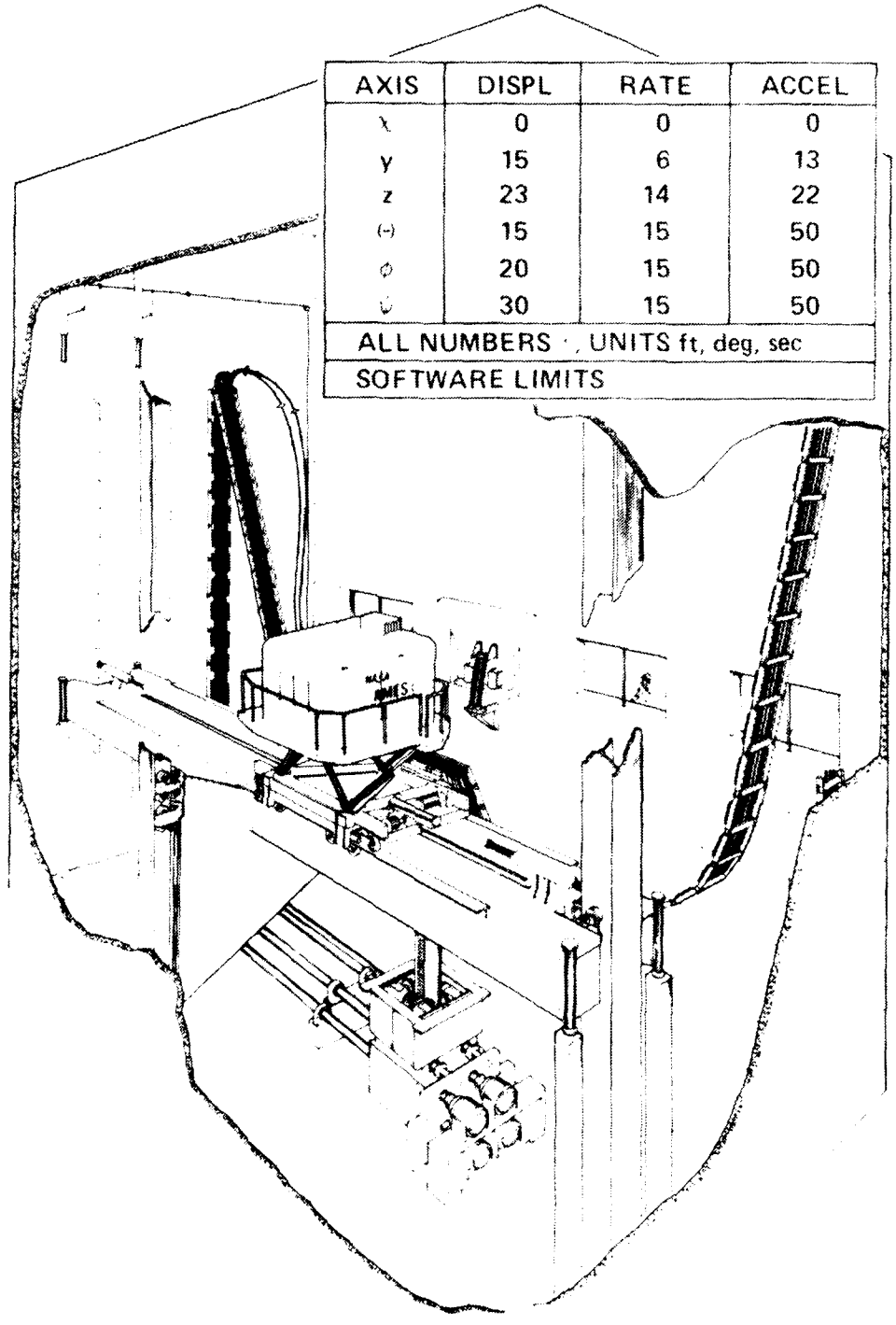

Figure 2.- Vertical motion simulator.

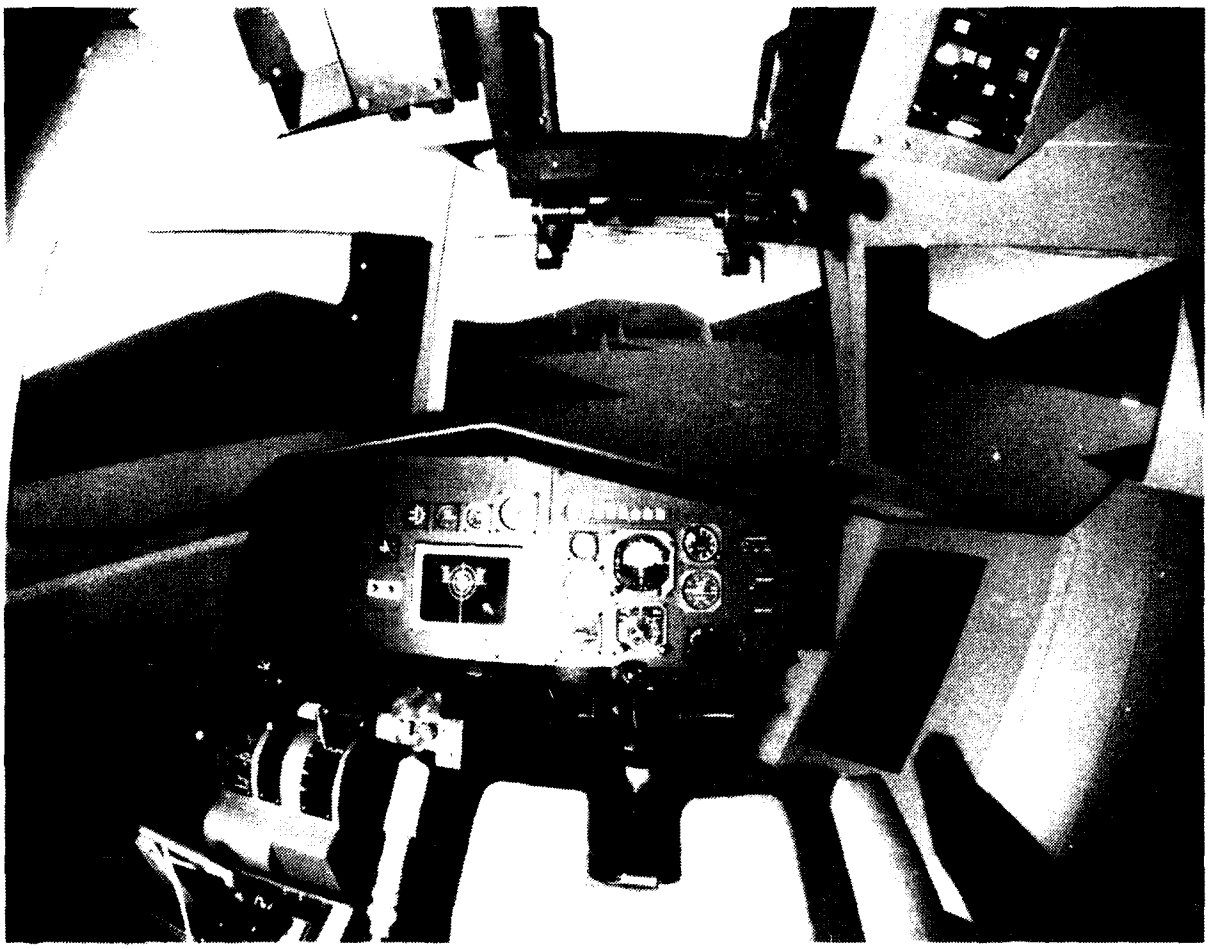

Figure 3.- Blue aircraft cockpit and computer generated imagery.

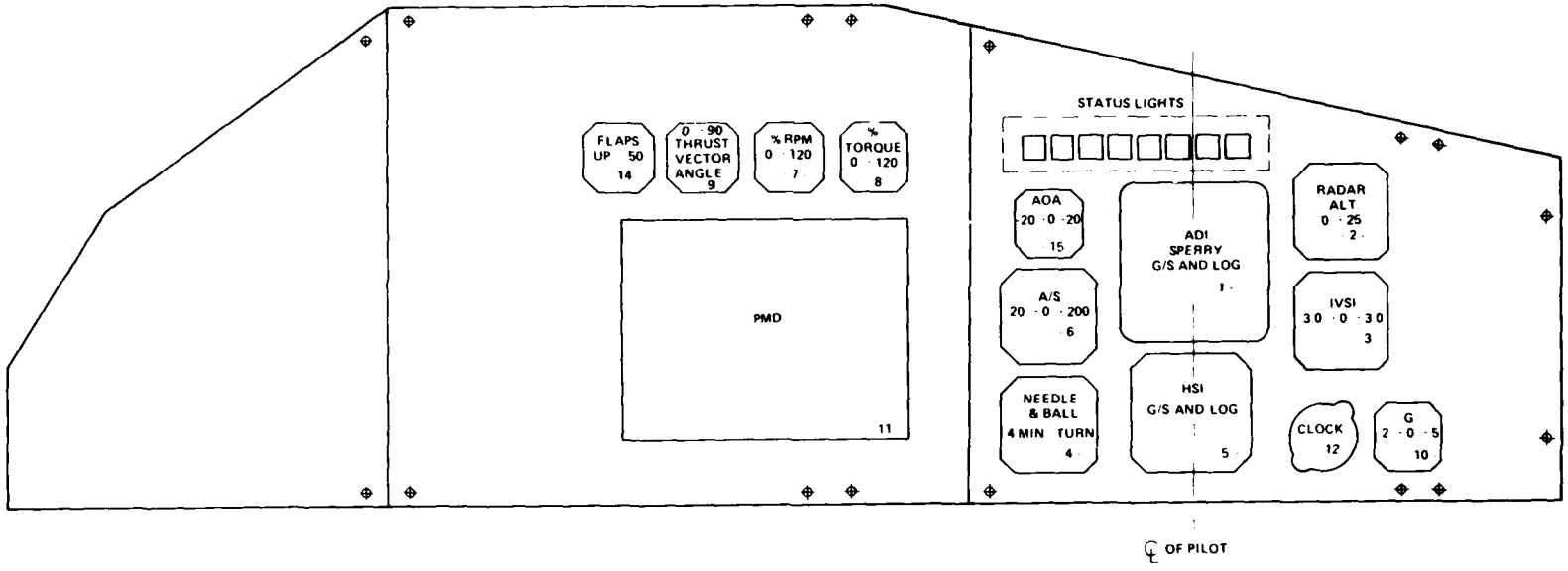

Figure 4.- Blue aircraft instrument panel.

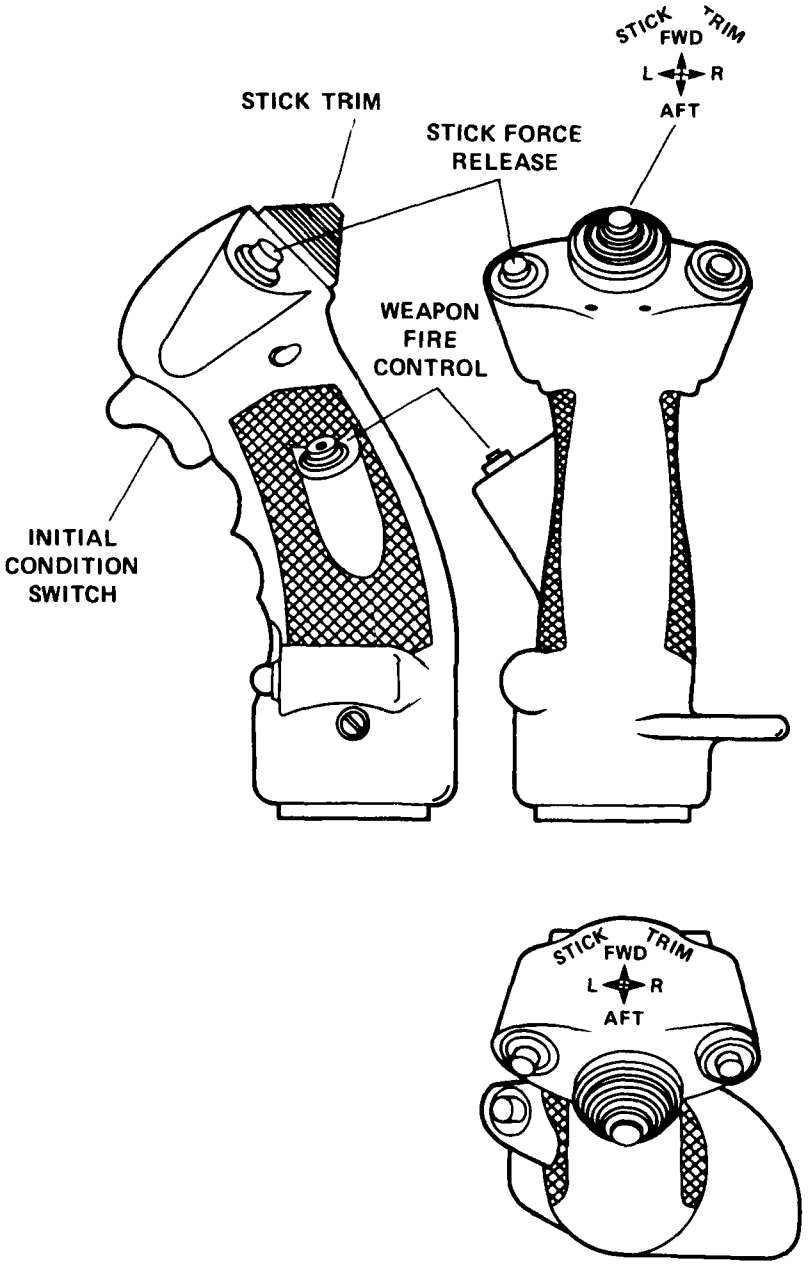

Figure 6.- Blue aircraft cyclic stick grip.

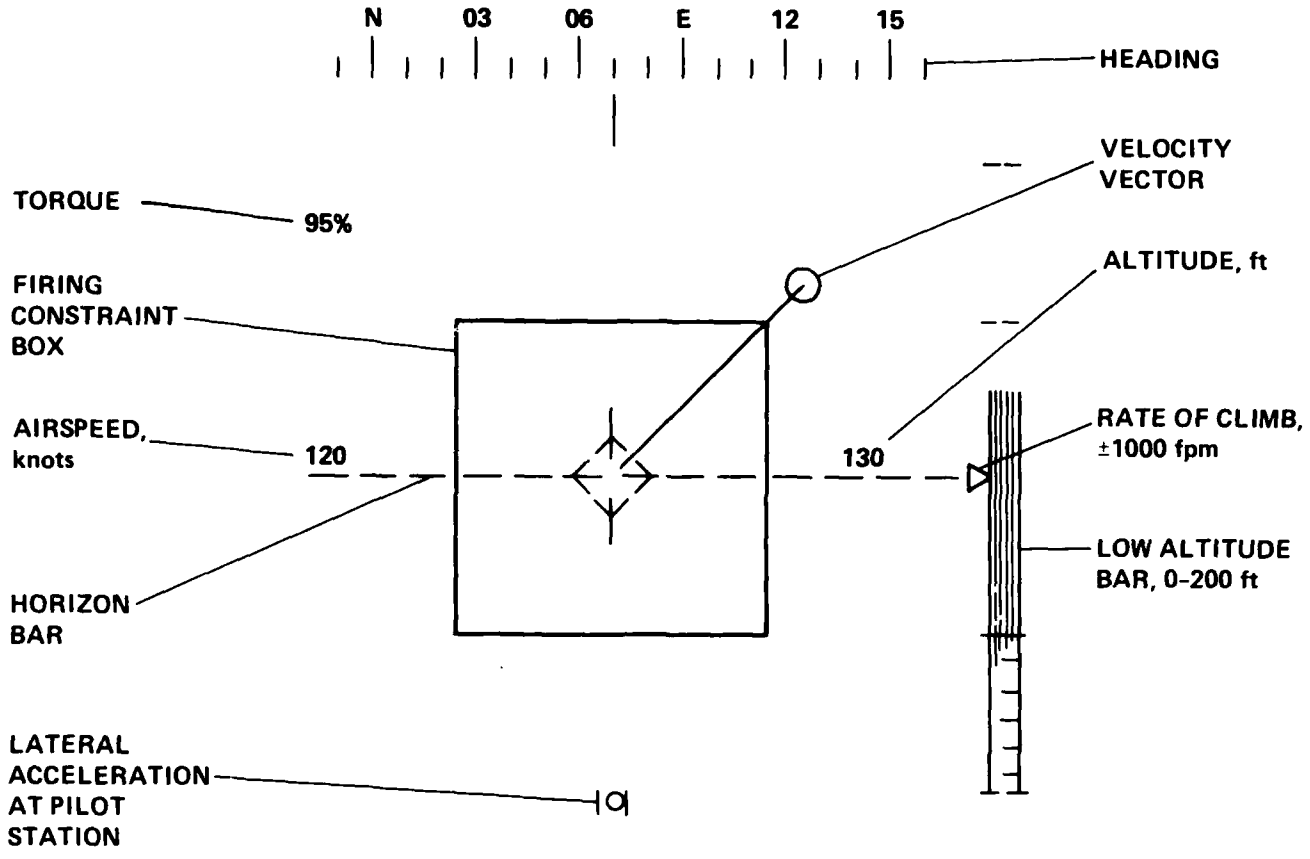

Figure 5.- Blue aircraft head-up display.

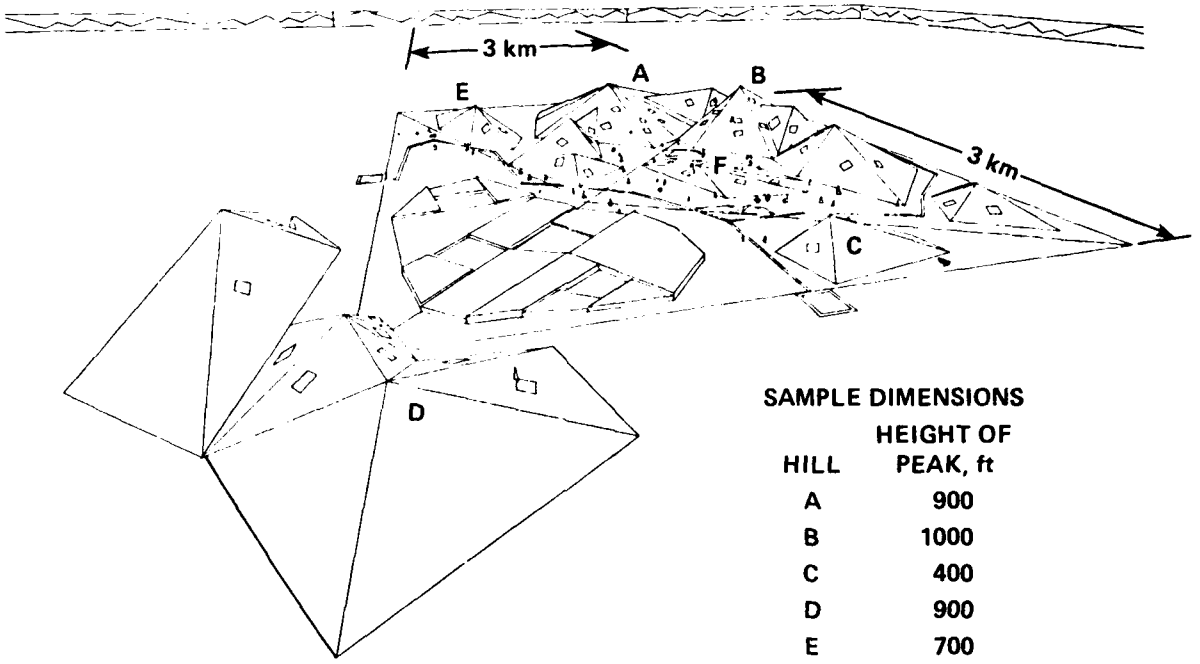

SAMPLE DIMENSIONS

HILL	HEIGHT OF PEAK, ft
A	900
B	1000
C	400
D	900
E	700
F	150

Figure 7.- CGI gaming area.

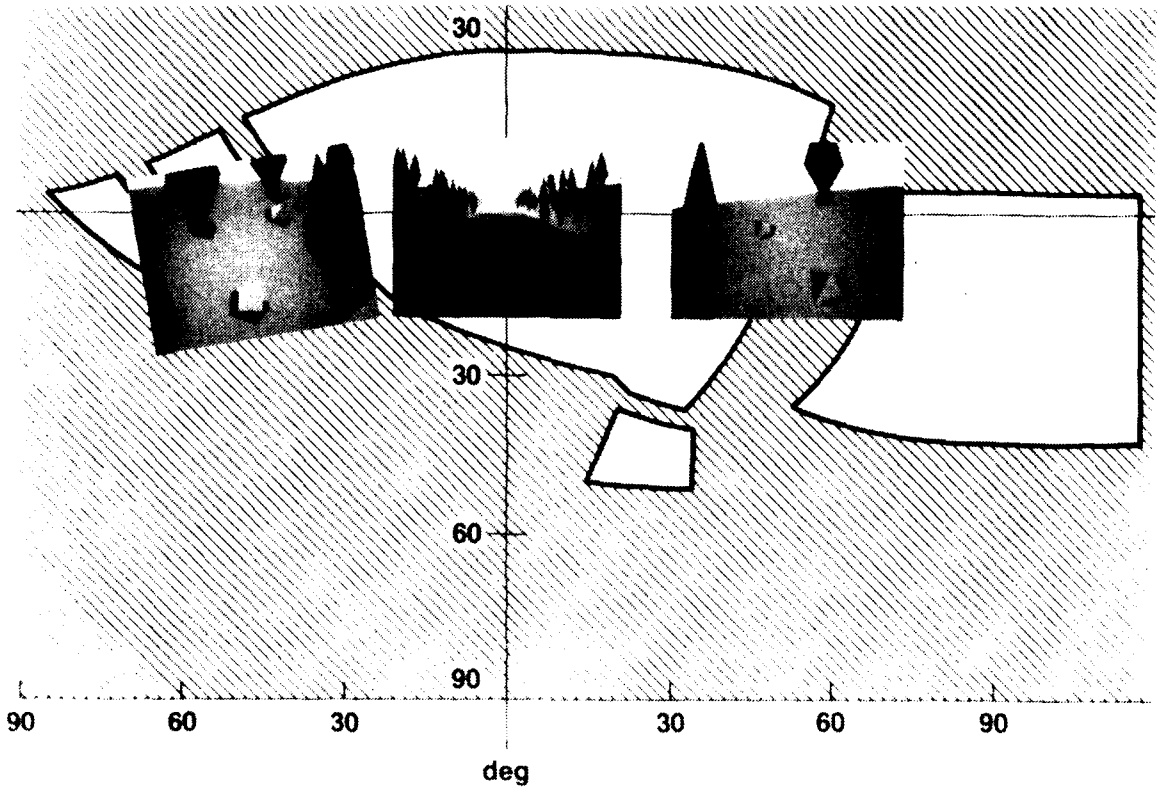

Figure 8.- Blue aircraft field-of-view.

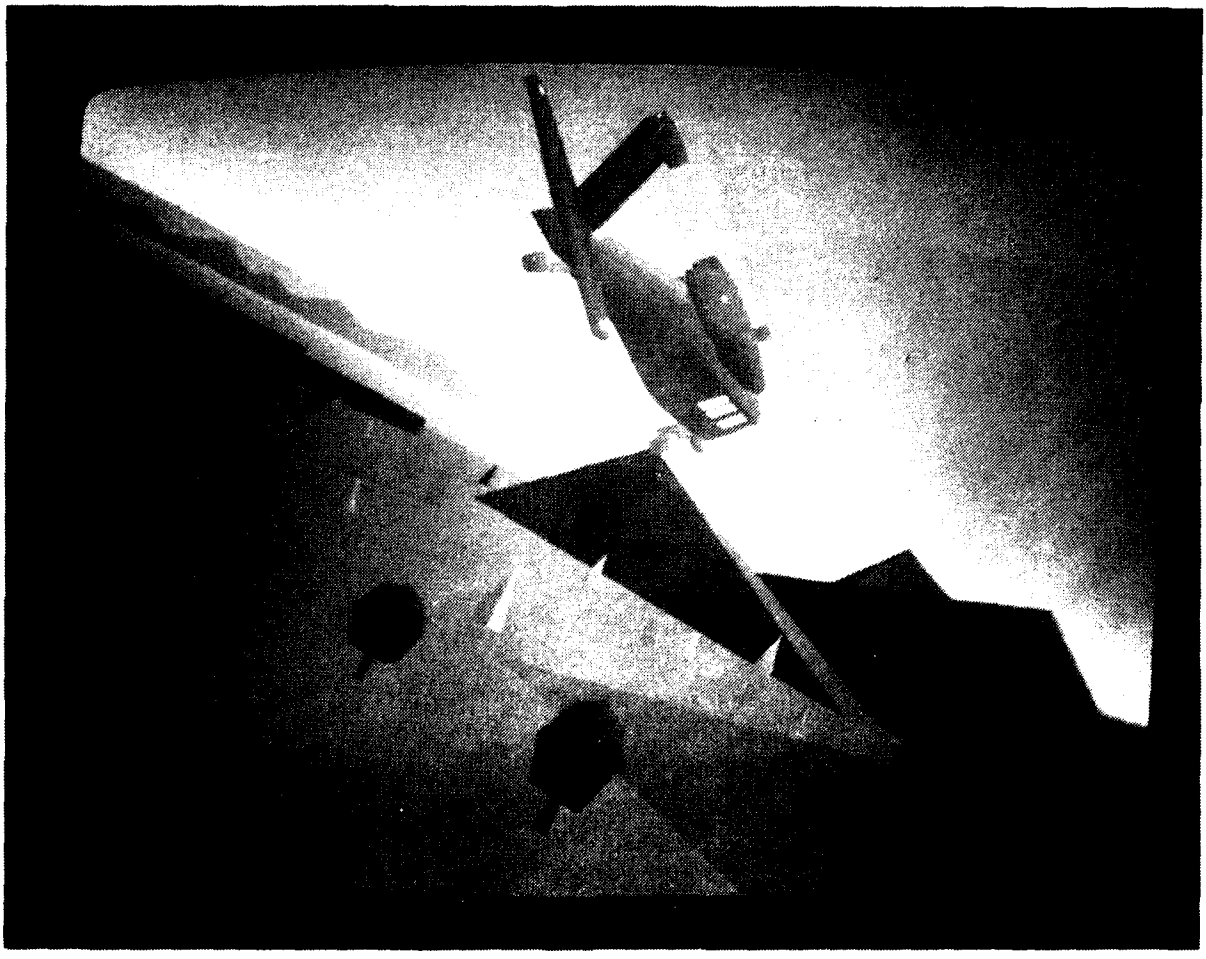

Figure 9.- Blue aircraft CGI.

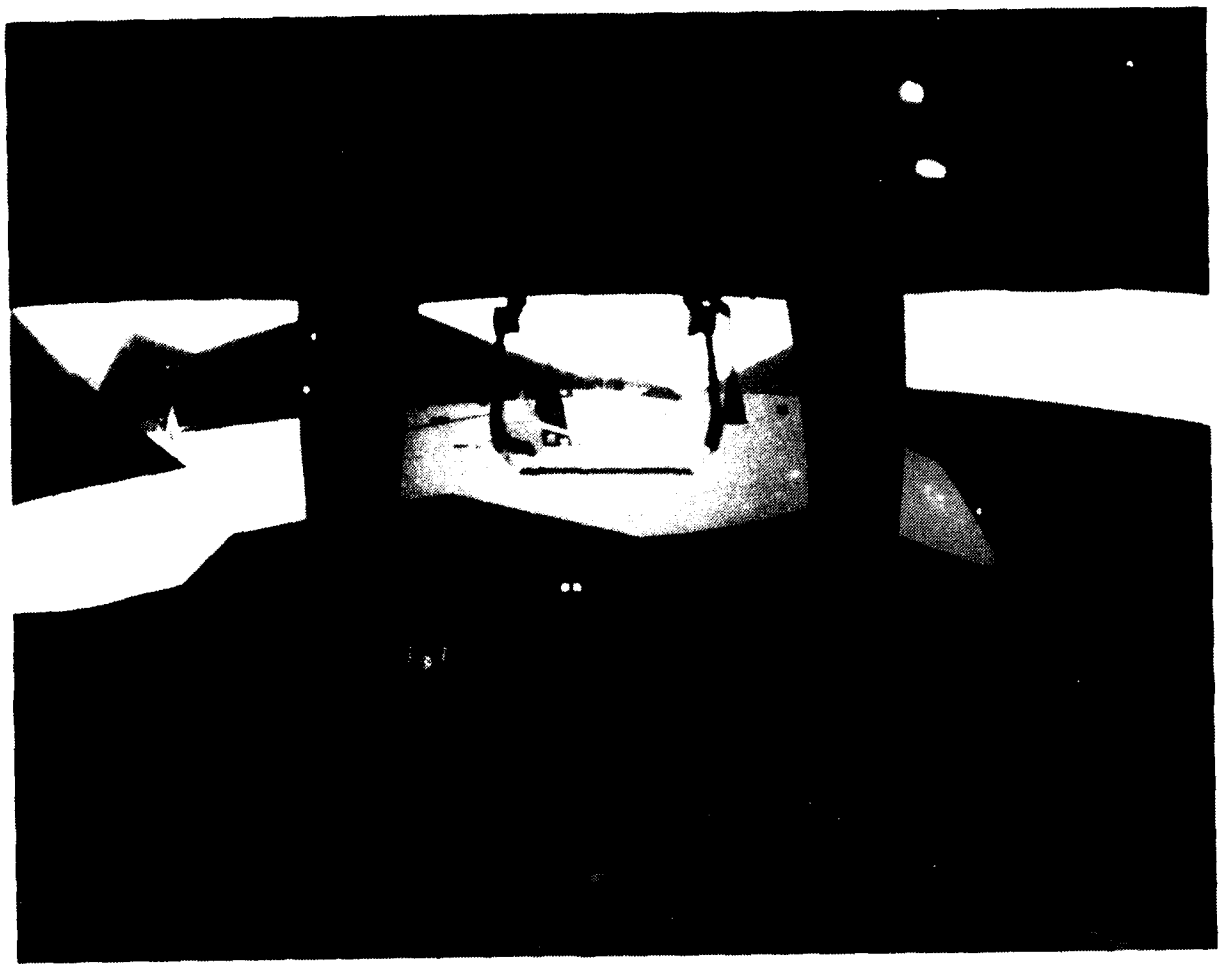

Figure 10.- Red aircraft CGI.

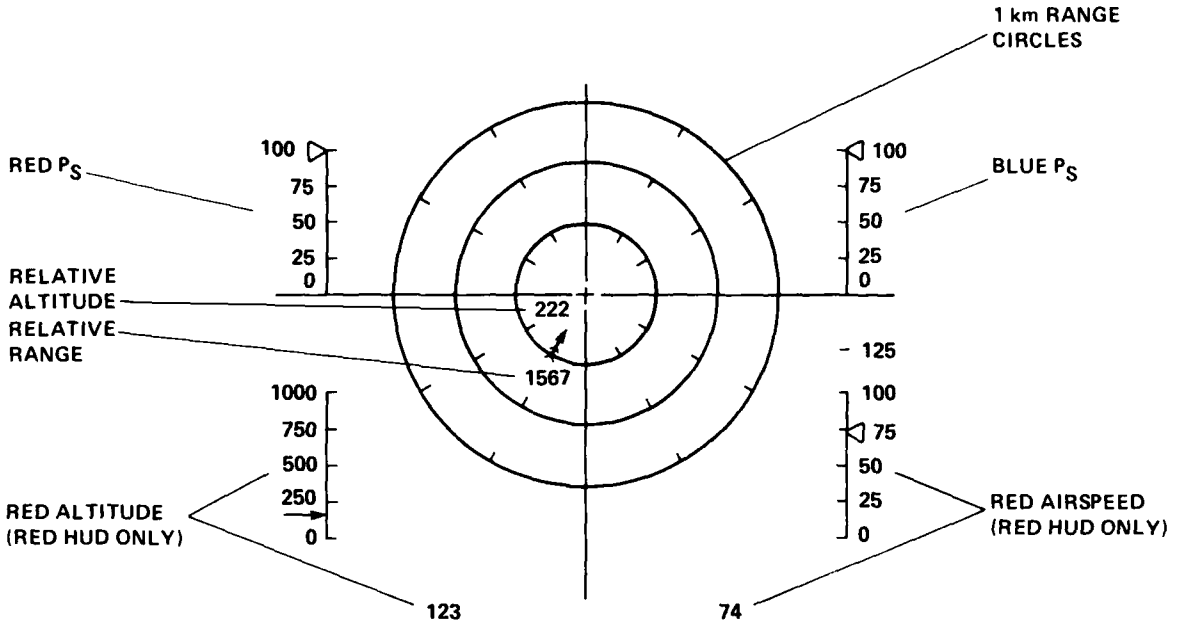

Figure 11.- Blue panel mounted display/red head-up display.

Figure 12.- VMS control room and red pilot station.

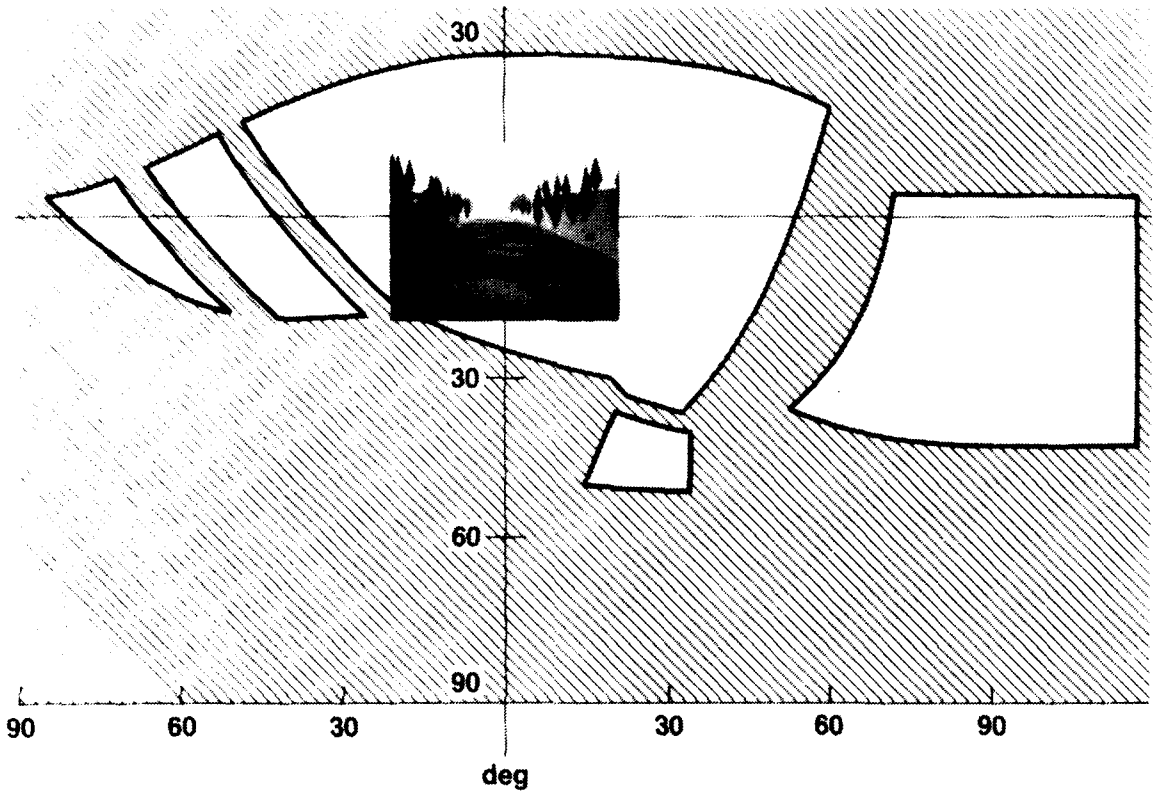

Figure 13.- Red aircraft field-of-view.

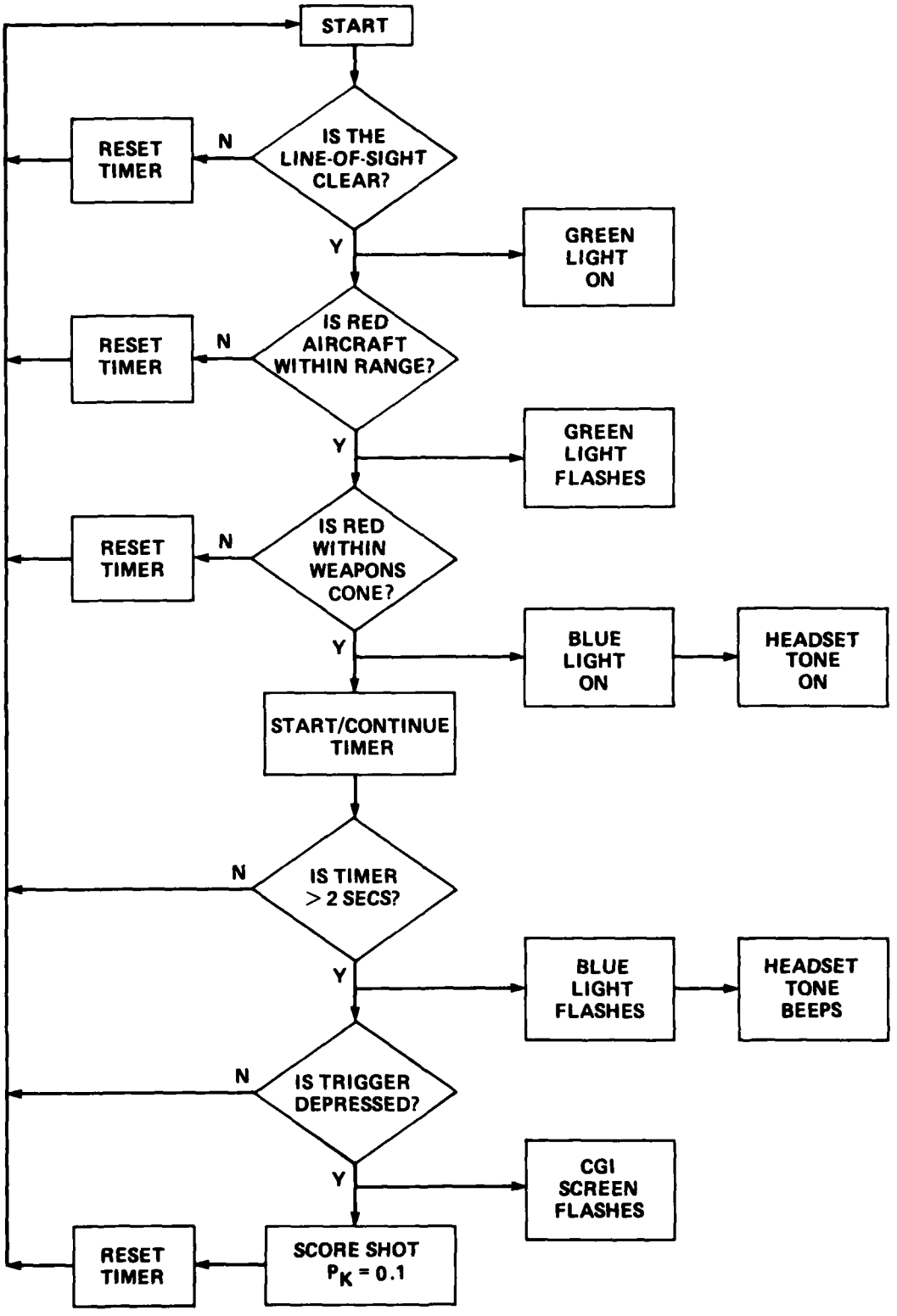

Figure 14.- Blue aircraft firing logic.

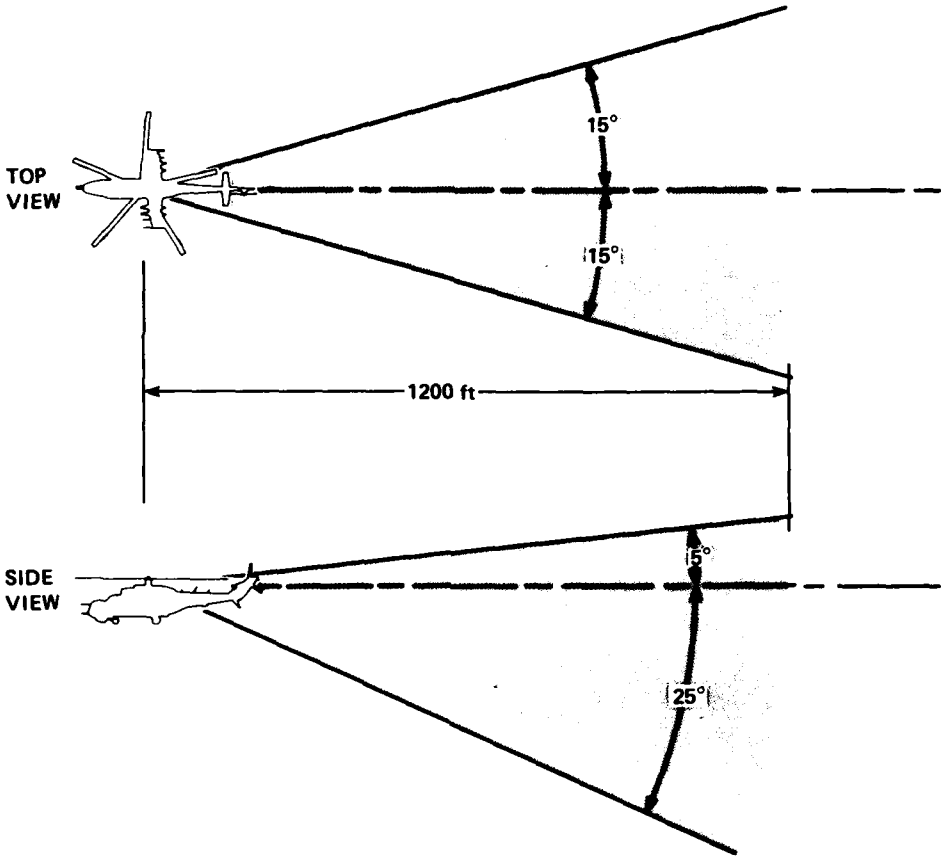

Figure 15.- Optimal tail chase cone.

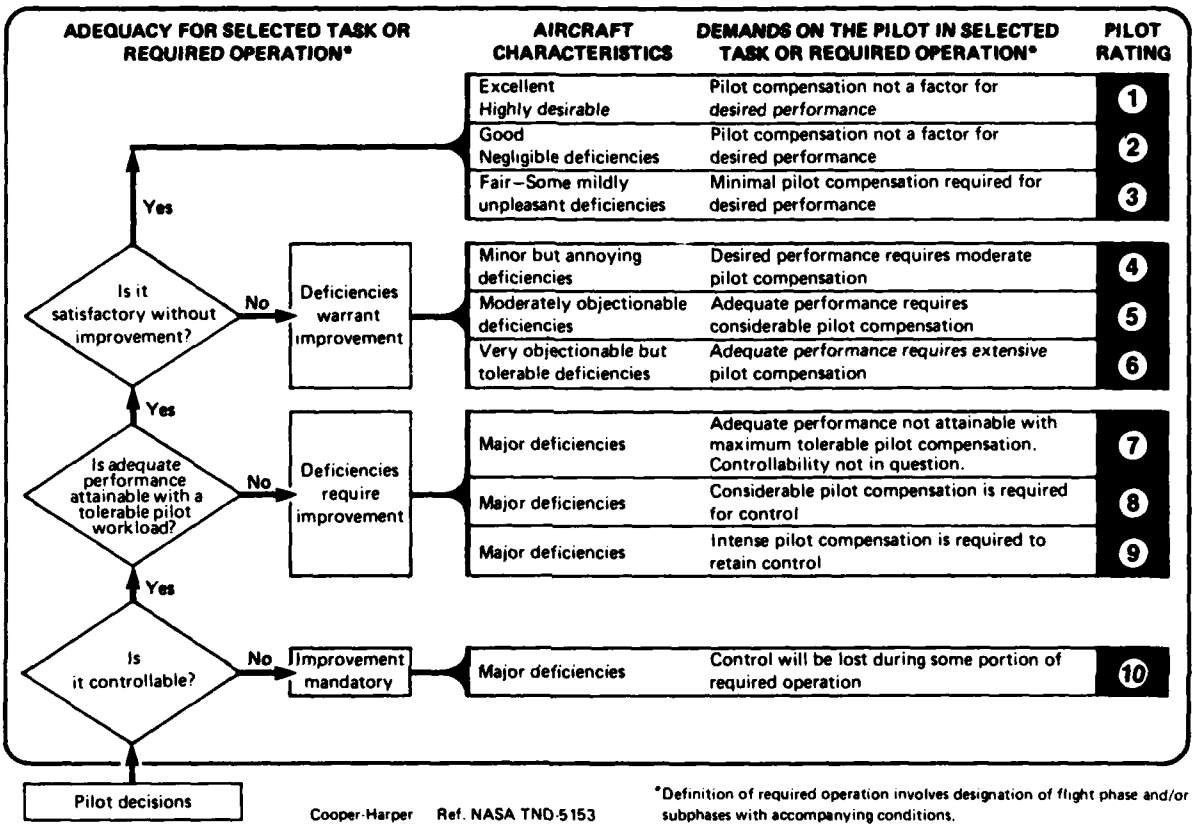

Figure 16.- Pilot rating scale.

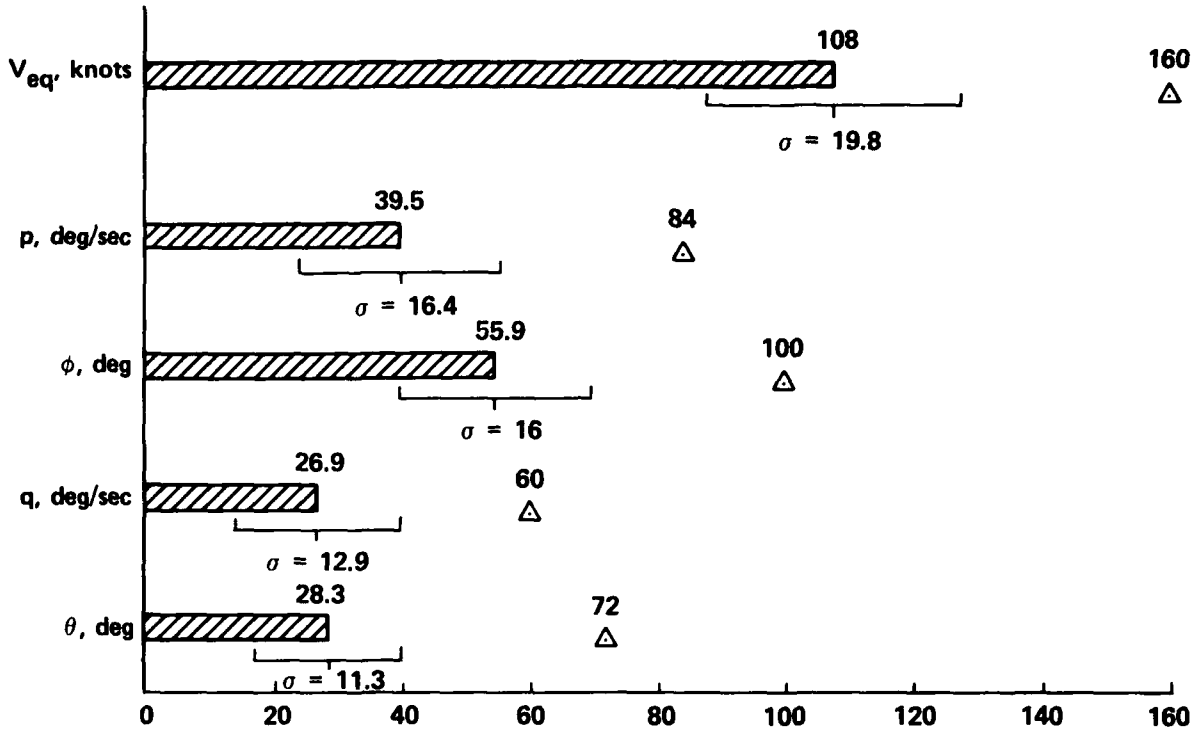

Figure 17.- Blue aircraft mean maximum angles and rates with agressive target.

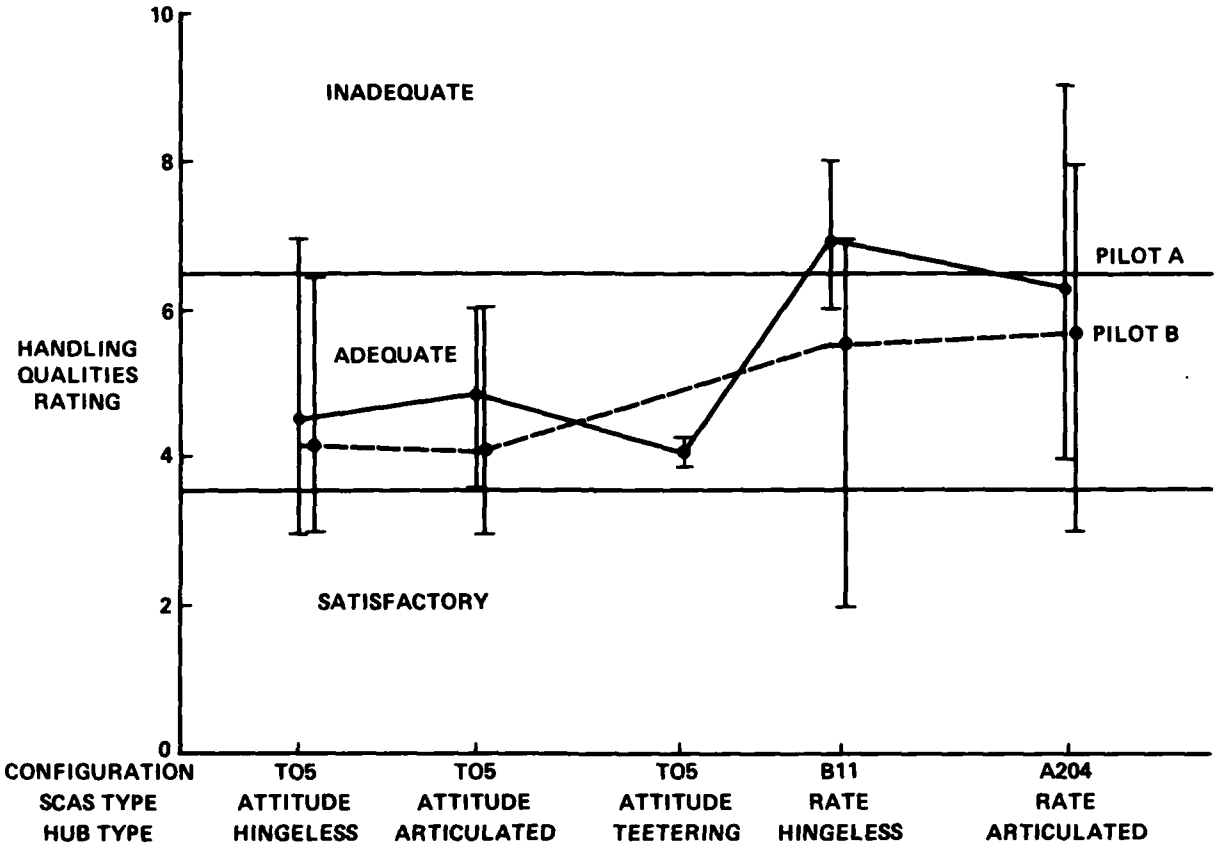

Figure 18.- Handling qualities rating vs configuration for combined aggressive target maneuvering runs.

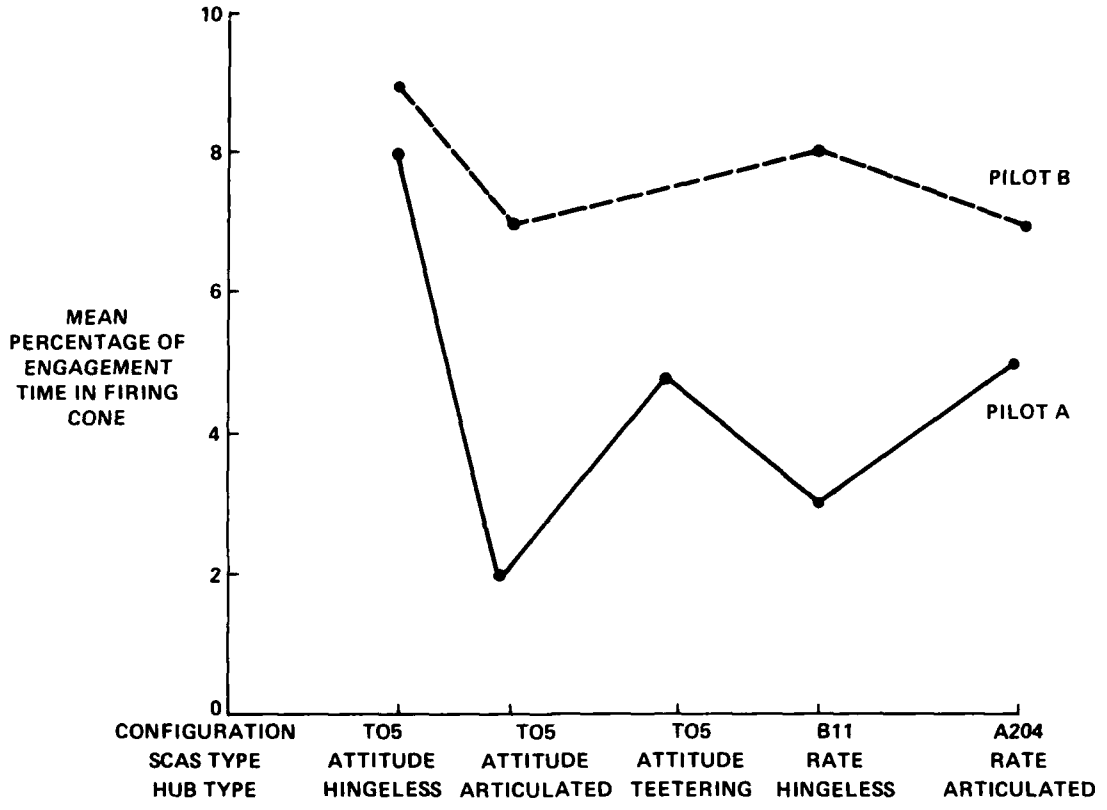

Figure 19.- Blue aircraft timer scoring vs configuration for aggressive NOE tail chase scenarios with nominal weapon characteristics.

AD A160538

1 Report No.	2. Government Accession No.	3. Recipient's Catalog No.
NASA TM 86686		

4. Title and Subtitle	5. Report Date
A PILOTED SIMULATION OF ONE-ON-ONE HELICOPTER AIR COMBAT AT NOE FLIGHT LEVELS	April 1985
	6. Performing Organization Code
7. Author(s)	8. Performing Organization Report No.
Michael S. Lewis and Edwin W. Aiken	85138
	10. Work Unit No.
9. Performing Organization Name and Address Ames Research Center and Aeromechanics Laboratory, U.S. Army Research and Technology Laboratories-AVSCOM, Ames Research Center, Moffett Field, CA 94035	11. Contract or Grant No.
	13. Type of Report and Period Covered Technical Memorandum
12 Sponsoring Agency Name and Address National Aeronautics and Space Administration Washington, DC 20546, and U.S. Army Aviation Systems Command, St. Louis, MO	14. Sponsoring Agency Code

15 Supplementary Notes

Point of contact: Michael S. Lewis, Ames Research Center, MS 211-2, Moffett Field, CA 94035. (415) 694-6115 or FTS 464-6115.

16 Abstract

A piloted simulation designed to examine the effects of terrain proximity and control system design on helicopter performance during one-on-one air combat maneuvering (ACM) is discussed. The NASA Ames Vertical Motion Simulator (VMS) and the Computer Generated Imagery (CGI) systems were modified to allow two aircraft to be independently piloted on a single CGI data base. Engagements were begun with the blue aircraft already in a tail-chase position behind the red, and also with the two aircraft originating from positions unknown to each other. Maneuvering was very aggressive and safety requirements for minimum altitude, separation, and maximum bank angles typical of flight test were not used. Results indicate that the presence of terrain features adds an order of complexity to the task performed over clear air ACM and that a mix of attitude and rate command-type Stability and Control Augmentation System (SCAS) design may be desirable. The simulation system design, the flight paths flown, and the tactics used were compared favorably by the evaluation pilots to actual flight test experiments.

17. Key Words (Suggested by Author(s))	18. Distribution Statement
Helicopter Rotocraft Air combat NOE Flight control systems	Unlimited Star category: 08

19 Security Classif. (of this report)	20. Security Classif. (of this page)	21. No. of Pages	22. Price*
Unclassified	Unclassified	52	A04

*For sale by the National Technical Information Service, Springfield, Virginia 22161

END

FILMED

12-85

DTIC